

Review article

Sutureless vascular anastomotic approaches and their potential impacts

Joseph G. Ribaud^a, Kevin He^a, Sarah Madira^a, Emma R. Young^a, Cameron Martin^a,
Tingying Lu^b, Justin M. Sacks^a, Xiaowei Li^{a,*}

^a Division of Plastic and Reconstructive Surgery, Department of Surgery, Washington University in St. Louis, MO, 63110, USA

^b Department of Plastic Surgery, Johns Hopkins School of Medicine, Baltimore, MD, 21287, USA



ARTICLE INFO

Keywords:

Sutureless

Vascular

Anastomotic device

Tissue adhesive

Patency

OUTLINE

ABSTRACT

Sutureless anastomotic devices present several advantages over traditional suture anastomosis, including expanded global access to microvascular surgery, shorter operation and ischemic times, and reduced costs. However, their adaptation for arterial use remains a challenge. This review aims to provide a comprehensive overview of sutureless anastomotic approaches that are either FDA-approved or under investigation. These approaches include extraluminal couplers, intraluminal devices, and methods assisted by lasers or vacuums, with a particular emphasis on tissue adhesives. We analyze these devices for artery compatibility, material composition, potential for intimal damage, risks of thrombosis and restenosis, and complications arising from their deployment and maintenance. Additionally, we discuss the challenges faced in the development and clinical application of sutureless anastomotic techniques. Ideally, a sutureless anastomotic device or technique should eliminate the need for vessel eversion, mitigate thrombosis through either biodegradation or the release of antithrombotic drugs, and be easily deployable for broad use. The transformative potential of sutureless anastomotic approaches in microvascular surgery highlights the necessity for ongoing innovation to expand their applications and maximize their benefits.

1. Introduction

Vascular anastomosis is a critical technique in multiple surgical disciplines, including cardiothoracic, plastic and reconstructive, and trauma. Vascular anastomosis allows surgeons to revascularize ischemic tissue and promote its survival. Consequently, it has transformed the healthcare field by providing life-saving options for many patients, such as those with myocardial infarction or those in need of dialysis. Vascular anastomosis has become a cornerstone of plastic and reconstructive surgery for its use in microvascular surgeries for flap transfer and tissue reconstruction. Plastic surgeons can take tissue from almost anywhere on the body and move it to another area, creating virtually endless possibilities of reconstructive surgery. However, microvascular anastomosis requires high skill level, resources, and cost, reducing its access substantially. Thus, a sutureless microvascular anastomosis alternative has potential to expand access of reconstructive surgery worldwide [1–3].

Sutureless anastomosis, a contrast to traditional suture-based methods, aims to shorten surgery duration, reduce post-surgery

complications, and enhance the success of vessel connections. This technique overcomes the issues tied to arterial elasticity and the complexities of suturing, paving the way for faster recoveries and minimally invasive surgeries. The concept of sutureless anastomosis dates back over a century. The first experimentation of a sutureless anastomotic device was in 1897, when G.B. Quierolo implemented this technique during his studies of hepatic blood flow. Quierolo used a glass tube as a stent for portacaval anastomosis [4]. In 1900, Erwin Payr expanded on Quierolo's idea by using a magnesium absorbable tube. In 1904, Payr added pins orthogonal to the end of the tube, to secure the anastomosis in place [2]. Progress in sutureless anastomosis stagnated for years until World War II, where traumatic vessel damage became ubiquitous amongst fallen soldiers. Arthur Blakemore conducted sutureless arterial anastomosis using a vein graft with vitallium cuffing, claiming high patency rates [5]. However, this method led to many complications such as gangrene and amputation on the battlefield [6]. Weiss and Lam expanded on Blakemore's technique by using tantalum instead of vitallium with a vein graft lining the tube. This decreased thrombogenicity and increased patency at 2-month follow up. Their largest

Peer review under responsibility of KeAi Communications Co., Ltd.

* Corresponding author. Room 3308A, Clinical Science Research Building, Washington University School of Medicine, St. Louis, MO, 63110, USA.

E-mail address: xiaoweili@wustl.edu (X. Li).

<https://doi.org/10.1016/j.bioactmat.2024.04.003>

Received 11 January 2024; Received in revised form 25 March 2024; Accepted 4 April 2024

2452-199X/© 2024 The Authors. Publishing services by Elsevier B.V. on behalf of KeAi Communications Co. Ltd. This is an open access article under the CC BY-NC-ND license (<http://creativecommons.org/licenses/by-nc-nd/4.0/>).

predictor of failure was contamination and subsequent infection [4]. In the same era, Sidney Smith used an absorbable tube for vascular anastomosis to simplify suturing of smaller arteries and reduce intima damage during hand-sewn anastomosis [7]. Smith's experiments showed success, inspiring Swenson and Gross to use absorbable fibrin as a biodegradable tube for sutureless venous anastomosis [8]. In the 1950s, sutureless vascular anastomosis techniques evolved quickly. Takaro and Oteen used a stapling device for a prosthetic graft in dogs [9]. Peter Samuels introduced the concept of V-shaped vascular clips for quicker vascular repair [10]. By the mid-late 20th century, other pioneers were conceptualizing various devices such as lasers, magnets, and heat shrinking sleeves for sutureless anastomosis [11–13].

There has been substantial work in developing sutureless anastomotic approaches since the beginning of the 21st century. Specifically, the Global Excellence in Microsurgery (GEM) extraluminal coupler had great clinical results and was approved by the FDA in 2010 [14]. Furthermore, advancements in 3D printing technology and material science have provided direct printing of vascular anastomotic devices in biodegradable materials and metals [15]. The current research in thrombosis and vascular angiogenesis has also revolutionized device manufacturing, particularly by implementation of 3D fluid dynamic models [16].

It becomes clear that despite considerable progress in the field, substantial gaps remain in our knowledge and understanding necessary for a significant clinical impact [17]. A primary obstacle is that current approved devices for sutureless anastomosis necessitate vessel eversion, which is less suitable for arterial applications owing to the inherent increased elasticity of arteries. Unlike veins, arteries possess thicker media layers, enriched with a higher density of smooth muscle cells and elastin fibers. This structural composition confers arteries with greater elasticity, a crucial adaptation that protects them from rupturing under the high pressure conditions characteristic of the arterial vascular system. However, this increased elasticity coupled with a thicker media layer results in decreased compliance, presenting challenges for the effectiveness of existing sutureless anastomotic devices in arterial surgery [18].

In this review, we provide a comprehensive summary of the currently FDA-approved sutureless anastomotic devices, as well as those that are under investigation. We delve into the ongoing development of various approaches, such as couplers, stents, and tissue adhesives. For each approach, we present an overview of its mechanism, along with its respective advantages and disadvantages. We also discuss biological and biochemical factors that have posed challenges to the success of these approaches. There remains a gap that needs to be filled for a truly transformative sutureless anastomotic approach to revolutionize the field of microsurgery, particularly in arterial anastomosis.

2. FDA-approved devices

2.1. Global Excellence in Microsurgery coupler

The GEM flow coupler, developed by Synovis, is the only sutureless anastomotic device approved by FDA for microvascular anastomosis in free flaps. The coupler is specifically indicated for veins and arteries with a wall thickness of 0.5 mm or less and an outer diameter ranging from 0.8 mm to 4.3 mm. Functioning as an extraluminal device, it utilizes pins to penetrate the vessel wall (Fig. 1A). The device everts the vessel ends as they are pulled through, creating an intima-intima anastomosis secured in place by pins [19].

This device has demonstrated great results in venous anastomosis, exhibited by similar or improved patency and complication rates, while decreasing anastomotic time compared to hand-sewn technique. For example, Umezawa et al. analyzed end-to-side venous anastomosis cases using the GEM coupler. The GEM coupler reduced the anastomotic time significantly by 20 min compared to hand-sewn technique. Furthermore, complications requiring reintervention due to venous congestion were reduced in the GEM coupler cohort (2.7 %) compared to the hand-sewn cohort (4.5 %) [14]. In another study by O'Connor et al. the GEM coupler significantly decreased the failure rate of the venous anastomosis compared to the hand-sewn technique (1.4 % vs. 3.6 %) in microvascular breast reconstruction. Failures were considered if it required a revision, reasons including venous congestion and thrombosis. Notably, it also halved the anastomotic time, decreasing it from 21 min to 9.3 min [20]. Lastly, an economic study indicated that because of time saved in anastomosis, the use of the GEM coupler resulted in significant cost reduction [21].

Albeit the GEM device has shown success with venous anastomosis, its acceptance for arterial anastomosis remains limited. As described, the GEM coupler requires the eversion of the vessel over the pins. Arteries have thicker media layers than veins due to increased smooth muscle cells and elastin [26]. This promotes higher elasticity that prevents rupture in high pressured arterial vascular system. Increased elasticity and a thicker media lead to decreased compliance [18]. This inherent vascular nature of arteries makes them difficult to evert over the device. This has created much adoption hesitancy of the GEM coupler in arterial anastomosis [17,27]. For example, Pafitanis et al. showed that GEM coupler used in arteries yielded a success rate of 92 %. However, approximately 8 % of the arterial anastomosis required troubleshooting, including revision or conversion to hand-sewn anastomosis. The reasons for troubleshooting included thrombosis, wall rupture due to the device, arterial vessel thickness preventing eversion, and difference in arterial lumen sizes [27]. Nevertheless, the GEM coupler serves as a pioneering device in the field of microvascular surgery and validates many of the potential benefits associated with sutureless anastomosis (Table 1).

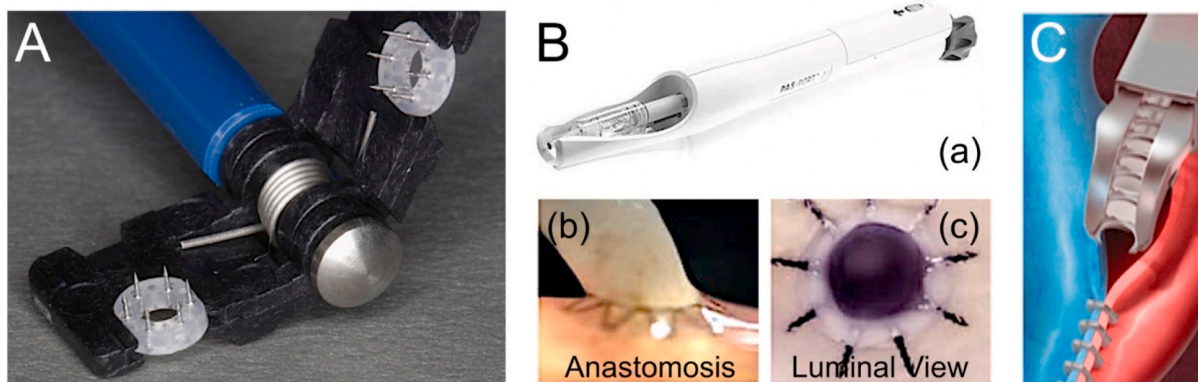


Fig. 1. Representative devices for vascular anastomosis. (A) GEM coupler. (B) PAS-Port system. (C) AnastoClip. The Figure is reproduced with minor adaptations from Refs. [22–25] with permission.

Table 1
Characteristics of various devices for vascular anastomosis.

Devices	Vessels	Advantages	Disadvantages	References
GEM Coupler	Veins	<ul style="list-style-type: none"> • FDA-approved (Clinical trial ID: K132727) • Comparable patency and complication outcomes to hand-sewn technique • Extraluminal nature limits inflammatory and thrombogenic response • Easy to use and time saving 	<ul style="list-style-type: none"> • Required eversion of vessels, limiting to venous use • Pin piercing poses potential for long lasting vessel damage 	[14,17,20,27]
PAS-Port System	Veins	<ul style="list-style-type: none"> • FDA-approved (Clinical trial ID: NCT00355563) • Significantly decreased anastomosis time • Patency and complication rates comparable to hand-sewn technique for calcified aortic anastomosis 	<ul style="list-style-type: none"> • Used in CABG procedures, not suitable for microvascular anastomosis • Required vessel eversion limits its use to veins 	[23,28]
AnastoClip	Arteries and Veins	<ul style="list-style-type: none"> • FDA-approved (Clinical trial ID: NCT01669850) • Interrupted suture technique, allowing for close mimicry to hand-sewn anastomosis 	<ul style="list-style-type: none"> • Difficult to use due to need for symmetric eversion • Conflicting clinical success rates 	[29–33]
InterGraft	Veins	<ul style="list-style-type: none"> • Under clinical trial (NCT02532621) • Quick, easy AV access for hemodialysis • Similar patency and complication rates to hand-sewn technique 	<ul style="list-style-type: none"> • Limited to hemodialysis with AV fistula • Cannot be used with microvascular end to end anastomosis 	[25,34,35]
Extraluminal Devices	Veins	<ul style="list-style-type: none"> • Already validated in multiple clinical settings • Limited inflammatory and thrombogenic response • Can encompass a variety of materials and designs • Feasible customization and prototype testing 	<ul style="list-style-type: none"> • Requires eversion of vessels, limiting its use to veins 	[36–40]
Intraluminal Devices	Arteries and Veins	<ul style="list-style-type: none"> • Already validated in multiple clinical settings • Can be coated with antithrombogenic and antiproliferative drugs • Does not require eversion, promoting arterial use • Feasible customization and prototype testing 	<ul style="list-style-type: none"> • Required adhesive/glue to secure in place • Increased risk for thrombogenicity and restenosis • Required antiplatelet therapy while stent is exposed to blood 	[15,41–48]
Laser-Assisted Vascular Anastomosis	Arteries and Veins	<ul style="list-style-type: none"> • No any foreign object, limiting inflammatory response • Similar patency as hand-sewn technique • Using heat and a solvent to create weld that is as strong and non-penetrating as a hand-sewn anastomosis 	<ul style="list-style-type: none"> • Balance between damage to vessel and anastomosis by heat • Increased aneurysm formation • Requires a laser in the operating room • Each tissue has a different absorption potential, requiring different exposure times to laser for anastomosis 	[11,49–53]
Photochemical Tissue Bonding	Arteries and Veins	<ul style="list-style-type: none"> • Uses light to create a strong weld • Does not use heat like LAVA, thus poses no overheating risk • No aneurysm development 	<ul style="list-style-type: none"> • Increasing thrombogenicity • No successful long-term patency • Requiring specific light equipment in surgery 	[54,55]
Vacuum-Assisted Coupler	Veins	<ul style="list-style-type: none"> • No any piercing material, decreasing vessel harm • Decreasing anastomosis time 	<ul style="list-style-type: none"> • Low early patency rates • Requiring a vacuum in surgery • Extraluminal with only used on veins 	[56,57]

2.2. PAS-Port System

The PAS-Port system is a sutureless end-to-side anastomotic device specifically designed for coronary artery bypass graft (CABG) procedures. It received FDA approval in 2008. The device involves the eversion of the vein graft over the device, which is then deployed into the aorta. The device pushes the vein through the anastomotic hole, and fans out to create a clamp from the inside of the aorta (Fig. 1B), creating an intima-to-intima anastomosis [23]. This device has been shown to maintain patency and complication rates similar to hand-sewn anastomosis. Furthermore, it does not increase the risk of major cardiac events. Puskas et al. reported that the post-surgery percentage of patients without major cardiac events were 97.7 % for PAS-Port system, and 98.2 % for hand-sewn anastomosis. Major cardiac events were recurrent myocardial infarctions, primarily due to restenosis of the anastomosed vessel [28]. The PAS-Port System is mainly utilized in cases where aortas exhibit excessive calcification or present other conditions that make the hand-sewn technique challenging. Although this device has little utility in microvascular anastomosis, it highlights that sutureless devices can provide useful alternatives to hand-sewn techniques in patients with unfavorable conditions (Table 1).

2.3. AnastoClip closure system

The AnastoClip closure system, manufactured by LeMaitre, received FDA approval in 2018. The system deploys non-penetrating titanium staples into each of the vessels, creating a sutureless anastomosis (Fig. 1C). Prior to placement, the vessels must be symmetrically everted

for bleeding control and proper anastomosis. The staples are placed in a simple interrupted fashion, similar to hand-sewn suture placement. The AnastoClip is mainly used in arteriovenous (AV) fistula, venous grafting, and dural surgeries [29]. It reduces anastomotic time significantly, approximately 5–10 min compared to 25 min for hand-sewn anastomosis [30]. However, its acceptance and use in microvascular anastomosis are limited because of its requirement for symmetrical vessel eversion. This technique is challenging when dealing with calcified, atherosclerotic or thick arteries [31]. For example, Findlay et al. encountered two post-operative hemostasis complications in the patients that received AnastoClip closure for carotid endarterectomies. One resulted from the use of an incorrect clip size. The other resulted from the clip failing, leading to a large neck hematoma that required emergent surgery [32]. Furthermore, Donker et al. concluded that the AnastoClip did not significantly improve surgical time due to the delicacy needed to create symmetric eversion [33]. These unsuccessful findings, along with the challenges in creating symmetric vessel eversion, have limited the utilization of the AnastoClip in the field of microvascular surgery. Importantly, these challenges are also seen with other sutureless devices that rely on staples/clips for microvascular anastomosis (Table 1).

3. Sutureless anastomotic approaches undergoing development

3.1. InterGraft vascular anastomotic connector system

InterGraft vascular anastomotic connector system was developed to provide easier and immediate AV access for hemodialysis patients. This

system is composed of expanded polytetrafluoroethylene (ePTFE). Its arterial and venous side has flared ends respectively, allowing the graft to expand and secure itself within the recipient vessel. These connectors have a self-expanding nitinol framework to promote a tight anastomosis. A multicenter study from February 2018 to July 2021 enrolled 158 patients to assess graft implantation using this device for AV hemodialysis patients. All patients underwent the same treatment process: arteriovenous graft implantation utilizing a venous anastomotic connector to establish the venous anastomosis, while the arterial anastomosis is sutured conventionally. In typical procedures, both the venous and arterial graft anastomoses are completed with suturing. The device showed a 92 % cumulative patency, surpassing the pre-specified goal of 75 %. Additionally, primary unassisted patency was 60 %. Graft infections were observed in six patients, albeit unrelated to the device, with no cases of emergent surgery, significant bleeding, or pseudoaneurysm. The device thus demonstrated potential as a successful and safe method for hemodialysis venous anastomosis at the 6-month mark (Table 1) [25,34,35].

3.2. Extraluminal devices

Extraluminal couplers have gained significant attention since the successful development and deployment of the GEM extravascular coupler. Extraluminal couplers bring two unique advantages of decreased inflammation and minimal disturbance to natural blood flow. Due to its extraluminal nature, these devices are not exposed to blood and thus prevents an immune response. Furthermore, by not interfering with blood, these devices decrease likelihood of clots and injury to vasculature. The pitfall of these devices is embedded in required eversion of vessels. Arteries are significantly more elastic than veins, which promotes their ability to resist the bounding pressure from the heart. This elasticity prevents them from bending easily and thus makes an extraluminal coupler difficult to use with them (Table 1).

3.2.1. Magnetic couplers

Ventrica Magnet Coupler (VMC) emerged in the early 2000s as the prominent magnetic sutureless device for end-to-side anastomosis.

However, several early studies demonstrated less promising results, preventing its adoption. For example, a multicenter trial found the VMC was successful in 32/41 (78 %) of cases. Failure causes were as follows: 3 patients had anastomotic leakage due to improper tissue implantation of device, 5 patients were supposed to receive device but it could not be deployed due to improper vessel diameter measurements, and one patient had plaque formation [58–60]. Ultimately, VMC demonstrated that anastomosis with magnets is possible, but it requires substantial improvement in design to accommodate different arterial sizes and not alter natural arterial conformation. Recently, Lu et al. described an extraluminal rivet ring magnet anastomotic device [61]. This device comprises two pairs of magnetic rings and two rivet-like rings (Fig. 2A). These magnetic rings are crafted from sintered neodymium-ferrous-boron materials (Ti-NdFeB). The rivet-like rings, 3D-printed from polyetheretherketone (PEEK), feature a 9 mm diameter base and a cylindrical structure (outer diameter 5.8 mm, inner diameter 4.8 mm, and height 1 mm) that can slide into the magnetic ring. They tested this device in end-to-end postcaval venous anastomosis in New Zealand rabbits (Fig. 2B). The device had faster surgery times than hand-sewn technique, and both groups showed similar anastomotic patency and postoperative outcomes at 12-week time point. There were no failures for their coupler. The hand-sewn cohort had two failures: one rat developed stenosis at the anastomotic site and one rat developed an obstruction. The device's anastomotic intima was smoother based on histology, likely an effect of suture damage to the intima in the hand-sewn group (Fig. 2C). This study demonstrated the potential of magnetic couplers as sutureless anastomosis devices [61]. However, magnetic couplers require vessel eversion due to their extraluminal nature, limiting usage to only veins. Another disadvantage is magnets placed inside of one's body can interfere with future medical procedures, such as magnetic resonance imaging (MRI). Also, the anastomotic strength hinges on the magnetic force and stability over time, which has not been extensively studied [62].

3.2.2. Plastic couplers

Recently, Li et al. have employed a unique extraluminal plastic coupler design. This coupler consists of one ring made from high-density

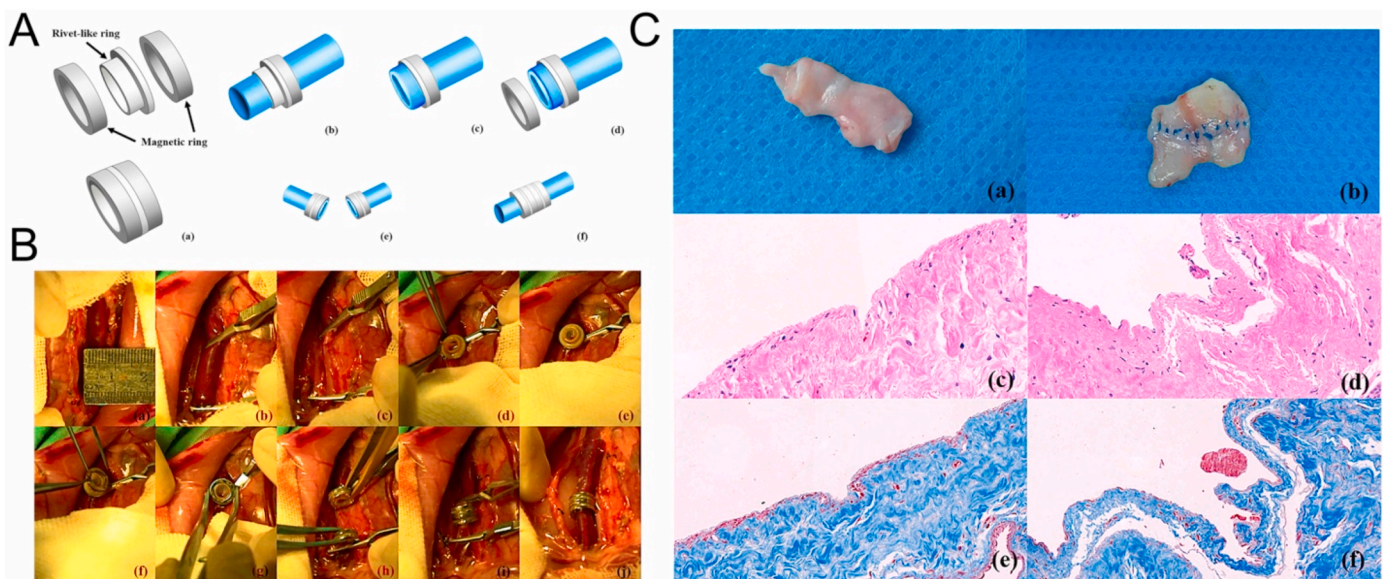


Fig. 2. Magnetic compression device for vascular anastomosis in rabbits. (A) Mechanism of the magnetic anastomotic device, including a two-magnetic-ring and one rivet-like ring set, vessel end installation, eversion, magnetic ring application, and connection process. (B) Anastomosis procedure: showcasing postcaval vein exposure, clamping, disconnection, passing through the rivet-like/magnetic ring complex, vessel end eversion, magnetic ring assembly, device installation on the other end, and the completion of end-to-end anastomosis through magnetic attraction. (C) Comparative analysis 12 weeks post-surgery: gross appearance and histological examination (HE and Masson staining at $\times 40$ magnification) of portacaval anastomoses in the magnetic compression anastomosis group (a, c, and e) and the continuous-interrupted suturing group (b, d, and f). The Figure is reproduced with minor adaptations from Ref. [61] with permission.

polyethylene (PE), created through computer numerical control machining, and a second ring from polymethylmethacrylate by laser cutting. During the procedure, vessels are threaded through these rings and then everted. The rings engage in a locking mechanism characterized by grooves and arms. In a pilot study, the team successfully implemented this approach by inserting an expanded polytetrafluoroethylene (ePTFE) tubing into a porcine transected carotid artery using two of these couplers, achieving two end-to-end anastomoses. The success of the anastomoses was confirmed both by ultrasound and a two-week post-surgery MRI [39,63,64]. However, it is considerably bulkier than the vessels it connects and larger than existing vascular coupling devices, like the Synovis coupler. For instance, its external diameter surpasses 8 mm for 3 mm arteries, with a length of roughly 10 mm. Given that space is often at a premium in microsurgery, such a sizable coupler may be unsuitable, especially when multiple anastomoses are needed at one surgical location [64].

3.2.3. Absorbable couplers

Various polymers have been utilized in vascular anastomosis, benefiting from the customizability offered by 3D printing technologies. These polymers include polycaprolactone (PCL), poly (lactic-co-glycolic acid) (PLGA), poly (L-lactide) (PLLA), and poly (L-lactide-co-ε-caprolactone) (PLCL) [36,38,39]. They have been extensively studied for other medical devices and thus have proven a high degree of biocompatibility and success [65,66]. Each of these materials have exhibited different degradation characteristics *in vivo* (PCL: 24–36; PLGA: 0.5–8; PLLA: 18–60; and PLCL: ~6 months) [36,67–70]. Chemical modifications can further optimize their degradation profiles. Ideally, a biodegradable coupler should maintain its integrity until the vessel heals and then degrade rapidly to minimize chronic inflammation while ensuring a robust anastomosis. For example, Park et al. created a novel biodegradable extraluminal device using copolymers of different ratios of L-lactide to glycolide. This device, designed to maintain structural integrity for at least three weeks, comprises two inner rings over which vessels are everted and an outer ring for clipping/connecting them, thus forming the anastomosis. Tested in a mini-pig liver transplant model, the device achieved successful anastomosis in all subjects. A 4-month autopsy showed complete absorption of the device and intact anastomosis [71]. Jeong et al. introduced a unique extraluminal coupler named the “modified sleeve”, featuring an inner-outer ring design. The process involves everting the first vessel over the inner ring to form a cuff, then

covering it with the second vessel, and securing the structure with a compression-providing outer ring (Fig. 3). Their design consisted of rings made from PLGA and PCL. The outer ring was constructed using an O-design and a C-design (Fig. 3A). The C-design included a slit through the ring to increase flexibility. They tested these couplers using a jugular venous model in New Zealand rabbits (Fig. 3B). Results showed PLGA’s superior degradation within eight months, the efficiency of coupler methods over controls, and confirmed full patency across all coupler groups via ultrasonography. This design, contrasting the non-absorbable GEM coupler, minimizes risks with its ‘coupler-on-coupler’ approach and employs the modified sleeve technique to reduce thrombosis risks. Collectively, these studies underscore that while various polymers can facilitate successful anastomosis, the optimal choice of material depends on its mechanical properties and degradation profiles [36].

3.2.4. Titanium couplers

Metals are an attractive material choice for device because of their strength and durability. One type of metal that has been used for sutureless microvascular anastomosis is titanium. Titanium has high biocompatibility and non-corrosive properties, making it an attractive choice for medical devices that are in prolonged contact with the human body. An et al. created a titanium vascular anastomotic device (TVAD) that utilizes hooks and a coupling mechanism to secure the everted vessels and rings to each other, cementing the anastomosis (Fig. 4A) [37]. They tested this device in porcine jugular veins (Fig. 4B). The device remained patent without leaks at the 12-week time point. There was no vessel damage, the anastomotic site was fully reendothelialized, and no foreign body reactions were detected through histological analysis (Fig. 4C). However, titanium does not degrade and may have long-term restenosis. Future experimentation with this metal is required to determine long-term effects.

3.3. Intraluminal devices

Research on intraluminal stents dates to the early 20th century, and their application has since transformed healthcare management for diseases such as coronary artery disease, biliary outflow obstruction, and ureteral obstruction [72–74]. Early intraluminal stents were bare metal stents, which led to high restenosis rates (approximately 20–30 % of cases) [75]. To combat this, researchers have coated stents with antiproliferation drugs such as ridaforolimus, zotalimus, or

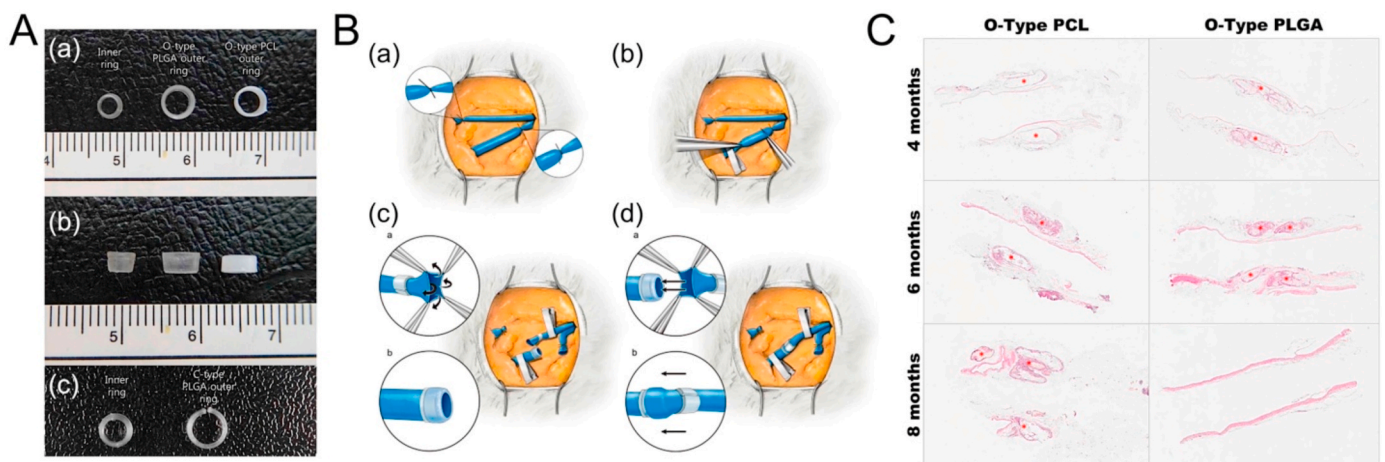


Fig. 3. Absorbable device as a modified sleeve technique for microvascular anastomosis. (A) O-type PCL, O-type PLGA, and C-type PLGA couplers. (a) Axial view showing O-type PCL with a non-slit PCL outer ring and PLGA inner ring, and O-type PLGA with a non-slit PLGA outer ring and inner ring. (b) Sagittal view detailing the tapered inner ring diameter, broadening away from the anastomosis site. (c) Axial view of C-type PLGA coupler featuring a slit in the outer ring for easier union due to PLGA’s stiffness. (B) Illustration of the modified sleeve technique for connecting external and internal jugular veins using the couplers. (C) Histologic analysis using Hematoxylin and eosin staining at 4 and 8 months, showing intimal layer remodeling and varying degrees of inflammatory response and degradation in both O-type PCL and PLGA couplers. The Figure is reproduced with minor adaptations from Refs. [36,64] with permission.

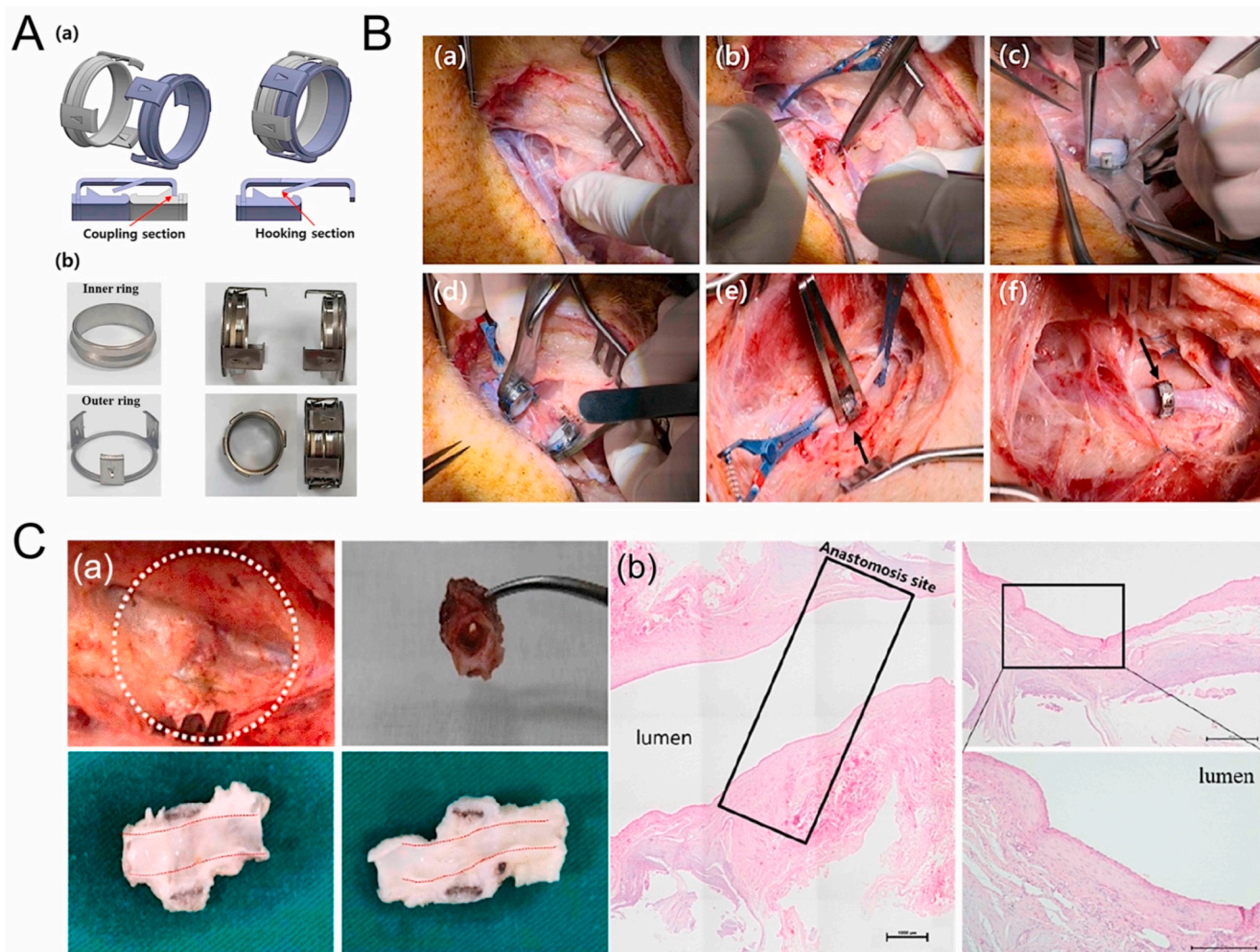


Fig. 4. Evaluation of a titanium vascular anastomotic device (TVAD) in pig jugular vein. (A) Design details of TVAD, highlighting its hooking and coupling components, and a photograph of the assembled device with its inner and outer rings, protrusions, and connecting arms. (B) Step-by-step intraoperative sequence of jugular vein anastomosis using TVAD: neck incision and vein exposure, vein clamping and division, vessel insertion into TVAD rings and hooks, and final coupling to form the anastomosis. (C) Postoperative assessment at 12 weeks: macro-photographic image and HE stained histological view, demonstrating successful attachment of TVAD to the vessel, no damage to the vessel lumen, complete endothelialization of the inner wall, absence of significant foreign body reaction, and clear intima-to-intima contacts at the anastomotic site (indicated by a rectangle). Figure is reproduced with minor adaptations from Ref. [37] with permission.

everolimus [41]. These drugs prevent smooth muscle proliferation and resulting restenosis [42]. Ultimately, intraluminal stents pose the unique advantage of not requiring vessel eversion. They are also easy to place, customizable to the vessel, and provide successful anastomosis. The disadvantage of intraluminal stents is increased risk of thrombogenicity and inflammation. They also require a glue or adhesive wrap to strengthen the anastomosis (Table 2). For a successful microvascular anastomosis using an intraluminal stent, researchers will need to minimize the inflammatory and thrombotic response by optimizing design, antiproliferative drug delivery, and stent material [76].

3.3.1. Metal alloy stents

Saegusa et al. 3D printed an expandable Microstent made from Nickel Titanium (NiTi) metal alloy. They chose NiTi because of its biocompatibility and its unique shape-memory ability. They utilized computational flow dynamics (CFD) to predict low areas of blood flow, which are catalysts for thrombosis. Based on their CFD findings, they optimized the number of branches and grip sizes of the Microstent. The optimal design consisted of 6 grips at each end, 12 branches, and a “Z” shape for the stent [15]. The resulting Microstent was tested in a rat lower abdominal aorta model. After placement, removal of a nylon

thread resulted in expansion and shape memory conformation. They circumferentially applied cyanoacrylate glue to further reinforce the anastomosis (Fig. 5A). Their results demonstrated significantly reduced operating time, while maintaining a tensile strength similar to hand-sewn technique. There were no associated thrombotic complications at 26 weeks (Fig. 5B). They attributed these decreased thrombotic events to their optimization of the grips and struts thickness, which decreased blood stagnation. Metal alloys provide unique advantages of biocompatibility, strength, and shape-memory, but they pose potential for restenosis if anticoagulation/antiplatelet drugs are not used [15].

3.3.2. Resorbable metal stents

Researchers also explored Magnesium (Mg) and Zinc (Zn) as resorbable metal stents for vascular anastomosis. Li et al. implanted a biodegradable Mg alloy stent (2 % aluminum, 1 % rare earth metals) in a venous graft model in New Zealand white rabbit (Fig. 6). They treated the Mg stent with both chemical conversion coating and polymer coating to decrease the degradation rate. The Mg stent promoted re-endothelialization and did not cause thrombosis, restenosis, or smooth muscle cell hyperplasia. Degradation of the stent began at 2 months, and complete degradation was achieved by 4 months [47]. However,

Table 2
Characteristics of tissue adhesives.

Tissue Adhesives	Adhesive Mechanism	Advantages	Disadvantages	References
Cyanoacrylates (Dermabond, SurgiSeal)	Polymerizing upon contact with tissue fluids to form strong, flexible bonds	<ul style="list-style-type: none"> •Great tensile strength •Setting quickly •Forming a waterproof barrier 	<ul style="list-style-type: none"> •Local inflammatory reaction •Brittle when dry •Not suitable for high tension areas or mucosal surfaces 	[95–97]
Fibrin Sealants (Tisseel, Evicel)	Mimicking the final stages of the coagulation cascade to form a fibrin clot, binding tissues together	<ul style="list-style-type: none"> •Forming natural clot formation •Hemostatic properties 	<ul style="list-style-type: none"> •Expensive •Low bonding strength •Potential risk of disease transmission 	[98,99]
Albumin/Glutaraldehyde (BioGlue)	Crosslinking albumin and tissue proteins by glutaraldehyde to form strong bonds	<ul style="list-style-type: none"> •Strong bonds •Hemostatic properties •Used in cardiovascular surgery 	<ul style="list-style-type: none"> •Potential tissue toxicity •Inflammatory reaction 	[102–104]
PEG Hydrogels (FocalSeal, Coseal)	Reacting with tissue proteins to form covalent bonds	<ul style="list-style-type: none"> •Biocompatible •Flexible for irregular spaces •Can be applied via endoscope •Moist environment for wound healing 	<ul style="list-style-type: none"> •Low bonding strength •More expensive •Degradation rate needs careful control 	[104,117]
Polyurethane-Based Adhesive (VIVO, TissuGlu)	Reacting with tissue proteins and moisture to form bonds	<ul style="list-style-type: none"> •Good flexibility •Biocompatible in certain formulations •Can be used in a variety of medical applications 	<ul style="list-style-type: none"> •Potential risk of inflammatory response •Some formulations may degrade •Not suitable for all tissue types 	[43,106,118]
Polysaccharide-Based Adhesive	Forming bonds through intermolecular attractions	<ul style="list-style-type: none"> •Biocompatible •Biodegradable •Derived from natural resources 	<ul style="list-style-type: none"> •Generally weak bond strength compared to synthetics •May not be as durable •Sensitive to moisture 	[110,111, 124–126,129]

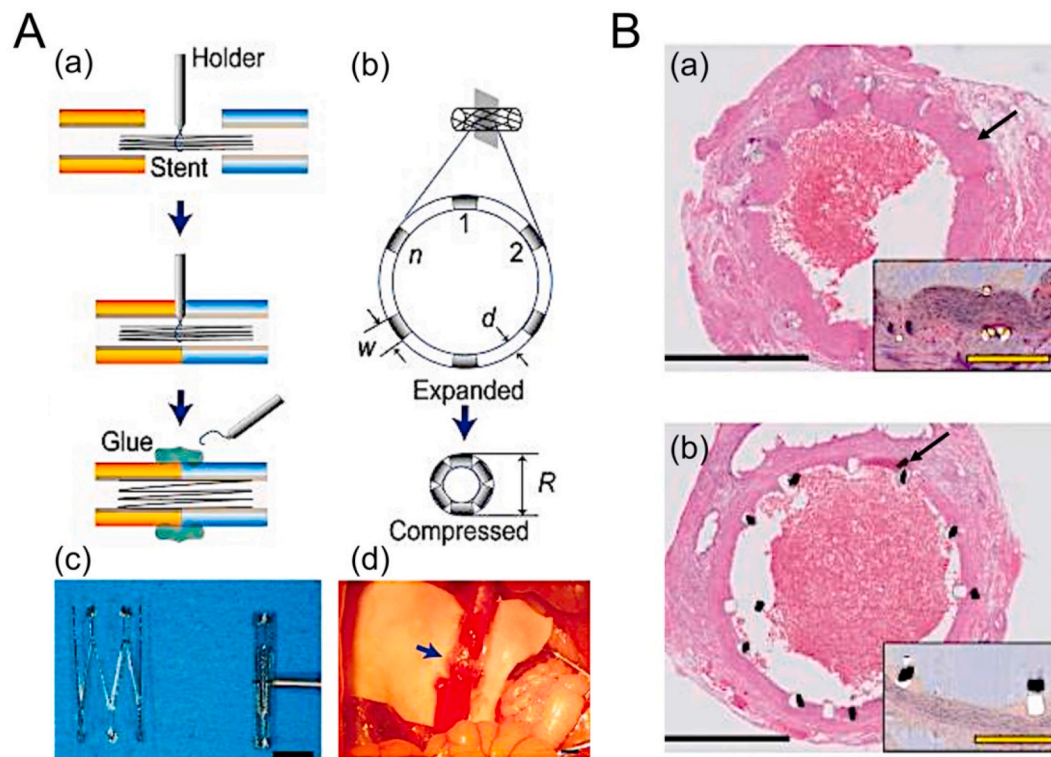


Fig. 5. Comparison of traditional and stent-assisted sutureless microvascular anastomoses. (A) Microstent design and implantation. (a) Microstent system for sutureless anastomosis, detailing stent compression, insertion, coaptation, expansion, and sealing with cyanoacrylate glue. (b) Calculation of compressed Microstent diameter based on branches, tube thickness, and width. (c) NiTi Microstent images showing fully expanded and compressed states, with a focus on the uniform Z-shaped branch arrangement. (d) Intraoperative anastomosis of rat aorta using Microstent, sealed with cyanoacrylate. (B) Histological analysis at 26 weeks post-anastomosis. (a) Hand-sewn rat infrarenal aorta with H&E and elastic Van Gieson stains, showing tunica media hyperplasia (denoted by arrow). (b) Microstent-anastomosed vessel exhibiting limited neointimal proliferation surrounding struts (denoted by arrow). Figure is reproduced with minor adaptations from Ref. [15] with permission.

untreated Mg has a high degradation rate, which if uncontrolled can lead to premature failure, decrease the local pH, and increase inflammation [77]. As a metal, Zn has a slower degradation rate than Mg, but

its mechanical properties, particularly tensile strength, are not as favorable. Mintegui et al. added Mg and copper (Cu) to Zn to examine effects on mechanical properties. Using Mg or Cu as an alloying element

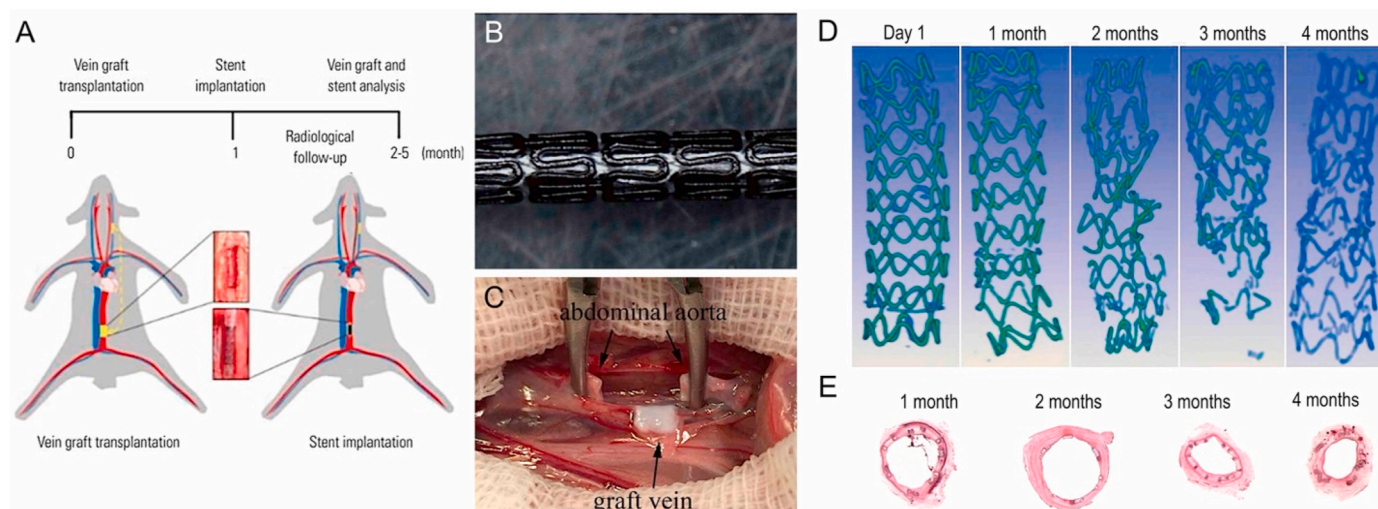


Fig. 6. Stent design and vein graft model. (A) Study design. (B) Demonstration of biodegradable magnesium alloy stents. (C) Surgery of vein transplantation. (D) Stent morphology by X-ray tomography *in vitro*. The continuity of the stent was gradually lost, and the contrast of the bracket has changed, which means the metal content had changed. (E) Hematoxylin and eosin staining showing a BMAS tissue section. Figure is reproduced with minor adaptations from Ref. [47] with permission.

significantly increased the ultimate tensile strength and yield strength compared to Zn alone [46]. Biodegradable metal stents provide strong anastomosis, can be altered to degrade within several months, and can be customized as alloys, coated with polymers or antiplatelet drugs. Despite these advantages, more experiments are needed to characterize the high corrosive rate and use *in vivo*.

3.3.3. Sugar stents

Sugar-based stents have emerged as a potential innovation in the field of medical devices, particularly in vascular applications [78,79]. Farzin et al. used 3D printing to develop a dissolvable sugar-based stent (Fig. 7). Their sugar solution contained glucose and sucrose, which were selected due to their biocompatibility and water solubility. In addition, glucose provided strong adhesion to vascular tissues. However, the main caveat of using glucose was its increased thrombogenicity, which was combatted by incorporating 3% sodium citrate. Sodium citrate is known to significantly decrease coagulation by chelating calcium. This novel stent material demonstrated low thrombogenicity (tested via *in vitro* clotting time assay). One of the most notable features of this sugar-based stent is its rapid disintegration time in aqueous environments, typically within 8 min. This property is particularly advantageous during hand-sewn anastomosis in surgical procedures. The quick dissolution of stent helps prevent acute inflammation and thrombosis post-surgery. However, its rapid degradation also imposes limitations on its use, making it suitable primarily for hand-sewn techniques rather than sutureless anastomosis. This highlights the role of stent as a temporary support structure rather than a long-term implant [45].

3.3.4. Vaso-Lock device

Recently, Gerling et al. tested the Vaso-Lock, a nonabsorbable, sutureless device with traction anchors that secure arterial ends, in a swine model involving femoral artery transection and repair. Unlike traditional methods, Vaso-Lock's anchors do not penetrate the vessel wall (Fig. 8). They exploit the natural elasticity of blood vessels to create a firm clamp. The device is made from implant-grade, antithrombotic polyetheretherketone (PEEK), which exerts frictional forces to connect arterial ends securely without vessel wall penetration. Its intraluminal design, chosen for stability and to minimize risks associated with absorbable materials, leverages the elasticity of arterial walls for a tight seal. The pilot study demonstrated the Vaso-Lock's technical feasibility over a 90-min period. Measurements of flow rates at proximal and distal ends of the 10 implanted Vaso-Lock devices showed consistent patency

without significant change or complications, suggesting its potential for vascular anastomosis procedures [80]. Currently, Vaso-Lock is indicated only for arterial use, as it has not been evaluated in venous systems. Comprehensive long-term performance and histological impact studies are still required for a complete assessment of Vaso-Lock.

3.3.5. Silk fibroin device

Silk fibroin, a blend of silk fibroin and glycerol, is a novel material for vascular anastomosis, offering both flexibility and strength, as well as being porous, oxygen and water permeable [81,82]. Jose et al. developed an anastomosis device using this material with a custom robotic system. The device features two parts: a cylindrical intraluminal coupler with spherical barb tips, made from silk and glycerol on Teflon-coated rods (150–300 μm thick), and a tubular sheath clip with a 250 μm thickness and holes for the barb tips (Fig. 9). These devices, requiring no harmful processing, exhibited high crush resistance, retention strength, and leak resistance, comparable to metal vascular implants. *In vitro* testing demonstrated that when the stent encountered fluid, it became softer, its outside diameter increased by 12%, and its wall thickness increased by 30%. These changes facilitate stent placement and improve vessel anastomosis because the stent is firm upon implantation, but then it becomes softer and expands with blood flow, creating a tight anastomosis. The device reduced the anastomosis time from approximately 20 min to less than 1 min. In a preliminary porcine study, the devices remained intact for 28 days, showing initial signs of degradation and cellular infiltration at component interfaces [48]. Other research groups have utilized silk fibroin scaffolds for vascular grafting and have demonstrated it promotes endothelialization [83,84]. While these results are promising, future development is necessary to manage neointimal tissue growth and adjust flexibility and permeability of the device.

3.4. Assisted approaches for vascular anastomosis

3.4.1. Laser-assisted vascular anastomosis

Laser-assisted vascular anastomosis (LAVA) has witnessed significant advancements since its introduction in 1979 [49,85]. Over the years, researchers have tested out various types of lasers, including CO₂, diode, and Argon lasers, in the context of LAVA. The physical properties of lasers, such as fluence, wavelength, and power, have been modified to affect tissue radiation exposure, anastomosis patency, and potential intima hyperplasia [11]. Achieving optimal laser anastomosis requires a

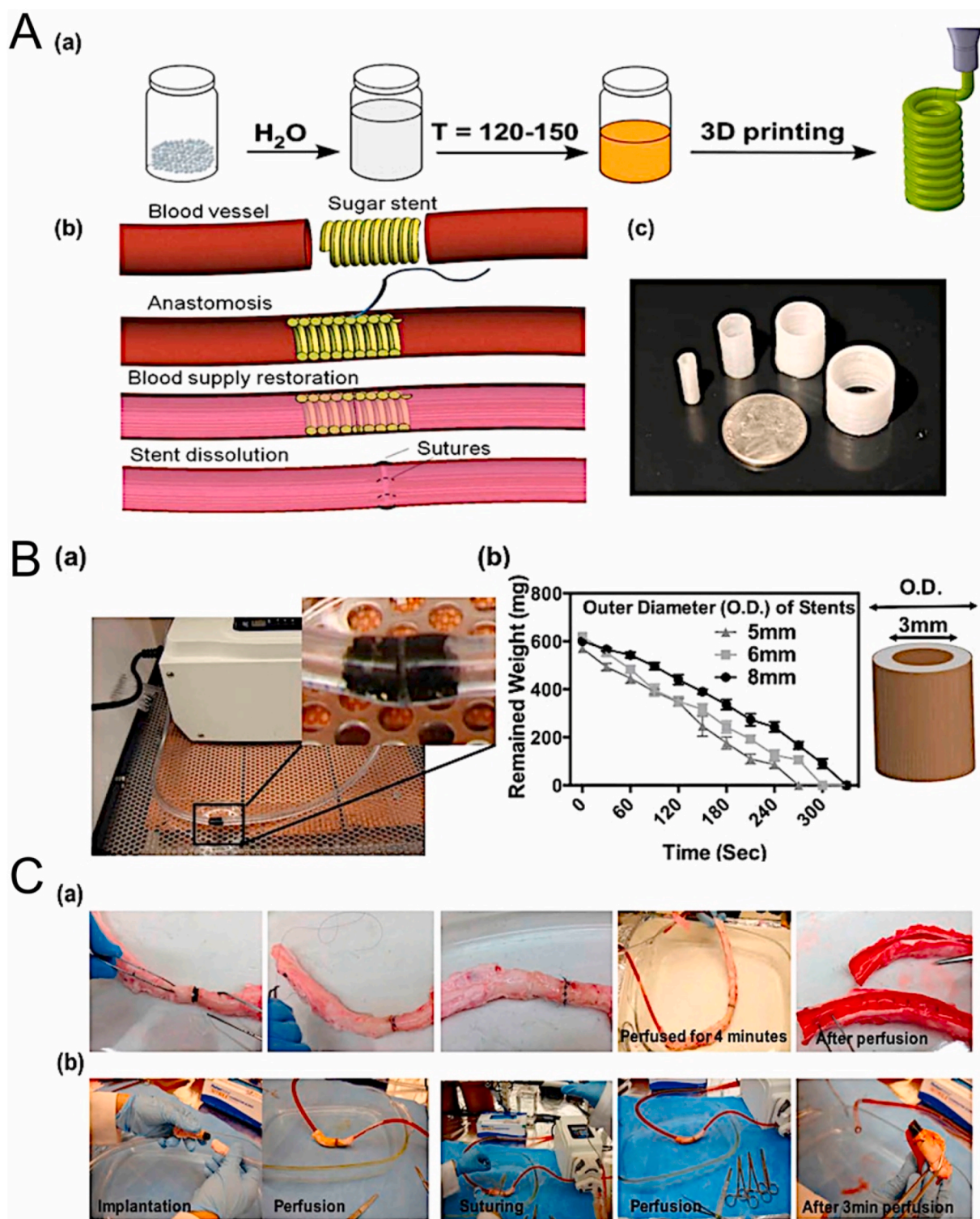


Fig. 7. 3D-printed sugar-based stents for vascular anastomosis. (A) Preparation and use of sugar-based stents in vascular anastomosis, including (a) 3D printing of sugar glass stents, (b) their application in surgical anastomosis, and (c) various dimensions of stents. (B) Dissolution rate assessment of stents, with (a) fluidic dissolution tests and (b) weight loss over time. (C) *Ex vivo* application in suture-based anastomosis with (a) rapid dissolution stents in pig arteries, and (b) longer dissolution stents, demonstrating no leakage during and after anastomosis. Figure is reproduced with minor adaptations from Ref. [45] with permission.

delicate balance of heat exposure sufficient to weld vessels together without causing excessive intima damage (Fig. 10A). Additionally, each tissue type has a predetermined absorption coefficient, impacting the amount of heat transmitted through the tissue during laser application. LAVA has shown to reduce occurrence of intima hyperplasia compared to hand-sewn anastomosis [50,51]. It has gained traction due to its ease,

speed, and minimal vessel damage, thus improving free flap surgery results by reducing flap ischemic time. A study compared traditional suturing with LAVA for orofacial defect reconstruction. Conventional methods averaged anastomosis in 19.8 min, while LAVA took 3.9 min. LAVA significantly reduced both anastomosis and ischemic times compared to traditional techniques [86]. Although these advancements

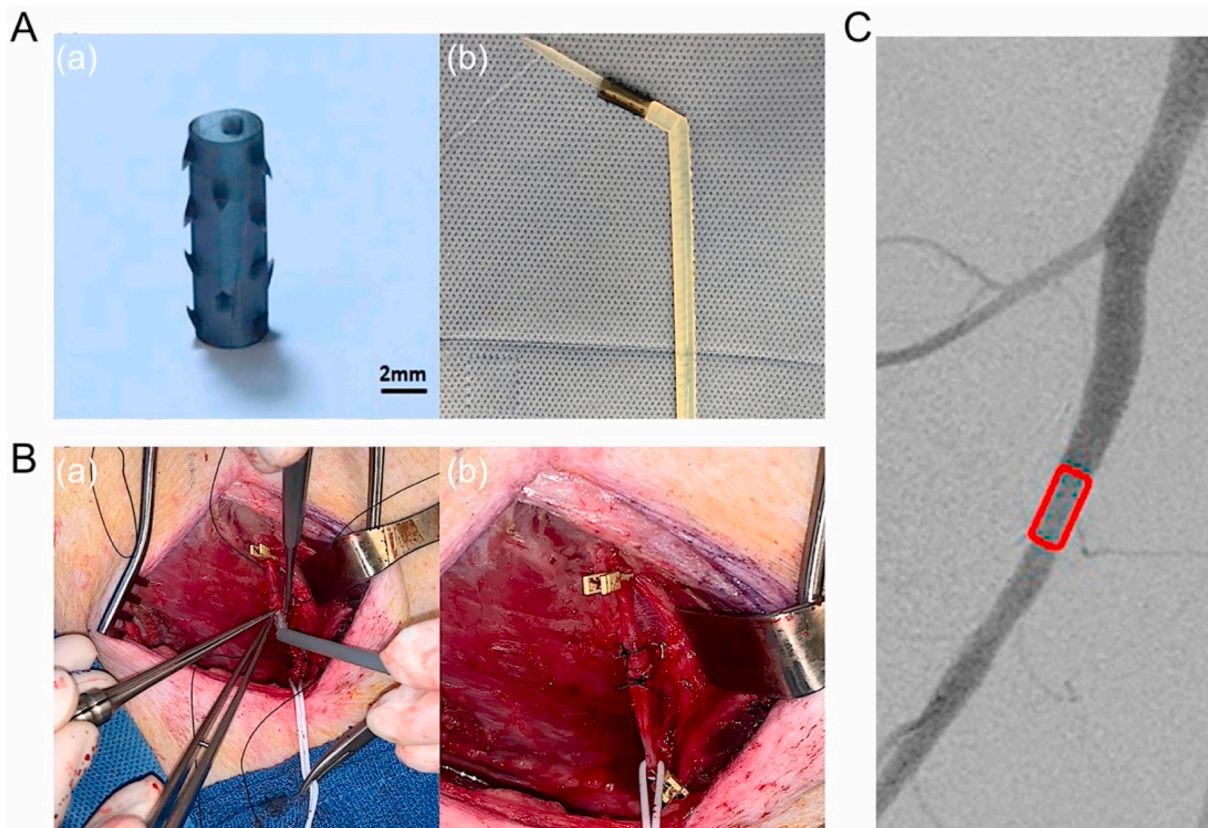


Fig. 8. Assessment of the Vaso-Lock anastomotic device in a swine model. (A) The Vaso-Lock apparatus presented outside of the body prior to insertion (a) and alongside the deployment instrument (b). (B) Placement of the Vaso-Lock at the beginning of the arterial segment (a) and the finalization of the anastomosis (b). (C) Final angiogram indicating unobstructed perfusion through the Vaso-Lock post-implantation, with the device's position marked by a red square. Figure is reproduced with minor adaptations from Ref. [80] with permission.

seem promising, the necessity for high laser equipment and extensive tissue laser absorption research hinders the adoption of LAVA to microvascular anastomosis (Table 1).

3.4.2. Photochemical tissue bonding

Photochemical tissue bonding (PTB) utilizes visible light to activate a photoreactive dye, leading to surface protein cross-linking and adhesion [55,87]. It has been used for wound closure in various tissues such as eye, peripheral nerve, tendon, colon, and skin. PTB is akin to LAVA, but without the accompanying heat damage, creating a robust bond between tissues (Fig. 10B). The main challenge with PTB is the need for an intraluminal stent to align vessels, which could lead to thrombotic complications. For example, Senthil-Kumar et al. employed PTB in femoral artery anastomosis in rats, initially observing patency rates equivalent to those of the hand-sewn control.

Thirty-five rats were divided into three groups for this study: Group 1 underwent standard suture repair (SR) with 10–0 nylon microsuture, Group 2 had standard suture repair with a stent (SR + S), and Group 3 received PTB repair with a stent (PTB + S). Initially, all vessels were open. By the end of one week, all SR group rats maintained patency, but only 5 out of 14 in the PTB + S group and 2 out of 8 in the SR + S group did so. They attributed the occurrence of thrombi to the long-term presence of the polyvinyl alcohol-based stent, as it was observed in both the photochemical (PTB + S) and non-photochemical tissue bonding (SR + S) groups [54]. A rapidly dissolvable stent should facilitate a light-activated microvascular anastomosis with excellent long-term patency. PTB offers a unique alternative for vascular anastomosis, but the need for stent placement and specific light equipment prohibits its widespread adoption (Table 1).

3.4.3. Vacuum-assisted microvascular coupler

The vacuum-assisted microvascular coupler (VaMAC) is designed with the aim of creating a sutureless anastomotic device that minimizes vessel trauma by avoiding permanent piercing the artery with pins. The VaMAC uses negative pressure to evert the vein over microspines, which are non-puncturing humps designed to securely hold the everted vein in place. The coupling device applies the same amount of pressure on both vessels, facilitating their eversion and subsequent creating a non-puncturing intima-intima anastomosis (Fig. 10C). Tachi et al. tested this device for end-to-side anastomosis in rats connecting the superficial epigastric vein to the femoral vein. The results revealed a low patency rate, with only 2 of 9 anastomoses remaining patent at the 1-week mark. The failed cases were attributed to clamp loosening [56,57]. Overall, the VaMAC is in an early stage of development, but large equipment requirements and unsuccessful preliminary trials impede its utilization in microvascular anastomosis (Table 1).

3.5. Tissue adhesives

Traditional methods for vascular anastomosis, primarily relying on suturing and stapling, often lead to complications such as tissue damage, inflammation, and the need for subsequent surgeries, especially in cases of large, critical wounds. Given these challenges, there is a growing inclination in the medical community towards advanced solutions, such as tissue adhesives, sealants, and hemostatic materials [88–94]. For example, cyanoacrylate adhesives, brands like Dermabond and Surgi-Seal, facilitate rapid bonding and microbial protection, though their inherent brittleness and cytotoxicity can pose limitations in vascular contexts [95–97]. Fibrin sealants, with Tisseel and Evicel leading the pack, emulate the clotting response of the body, offering flexible seals

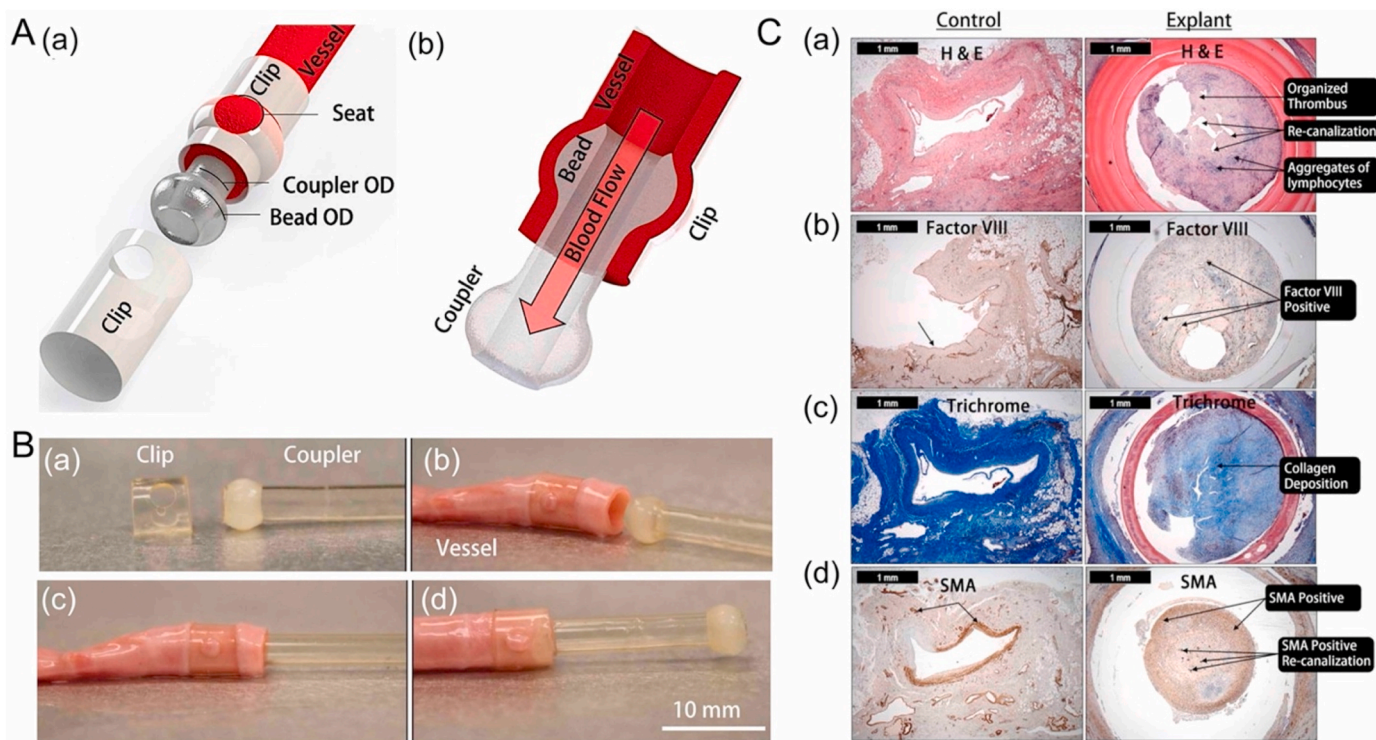


Fig. 9. Design and mechanism of self-curing silk fibroin anastomotic device. (A) Schematic of assembled components. Cross-section view of anastomotic device. (B) Method of anastomosis, first the clip was inserted over the vessel followed by inserting the coupler into the vessel. Finally, the clip is then slid toward the coupler and locked into place by aligning the seats over around the barbs. (C) Histology analysis. (a) H & E staining of the occlusion developed within the device (b) Factor VIII demonstrate the recanalization is lined with endothelial cells (c) Trichrome staining reveal collagen has been deposited within the occlusion (d) Cells within the occlusion and recanalization are positive for smooth muscle actin suggesting smooth muscle hyperplasia. Figure is reproduced with minor adaptations from Ref. [48] with permission.

particularly well-suited for internal vascular connections [98–100]. BioGlue combines bovine serum albumin with glutaraldehyde to form robust bonds, fortifying anastomotic junctions [101–103]. Polyethylene glycol (PEG) hydrogels, represented by FocalSeal and TissuGlu, boast adaptability and biocompatibility, making them valuable for the dynamic realm of vascular anastomosis [104,105]. Polyurethane-based adhesives add another dimension of choice in the anastomosis toolkit [106–108]. Furthermore, polysaccharide-based adhesives, derived from natural sugars, guarantee both biodegradability and biocompatibility, ensuring effective vascular seals with minimized inflammation [109–111]. For successful anastomosis, these tissue adhesives need to be optimized for biocompatibility, adhesive strength, and degradation in long-term studies [105,112]. Each of the adhesive solutions listed in Table 2 have benefits in some of these categories and limitations in others, further testing is needed to determine the ideal adhesive.

3.5.1. Cyanoacrylates

Cyanoacrylates were initially discovered in the mid 20th century. Initial versions irritated the skin and were not ideal for human use. Recently, more biocompatible versions, such as 2-octyl cyanoacrylate, present in medical adhesives like Dermabond. These formulations produce fewer toxic byproducts, promoting usage outside of the body. Although cyanoacrylates present advantages like rapid bonding and watertight seals, they also come with challenges, including brittleness, potential embolization, and high cytotoxicity inside the body [96,97]. Recent research explored the role of 2-octyl cyanoacrylate in vascular anastomosis using a rabbit carotid artery model. Ten rabbits underwent conventional anastomosis surgery with sutures only, while 10 underwent suture anastomosis, followed by the application of 2-octylcyanoacrylate. At 4 weeks, the adhesive group showed a notable reduction in the thickness of both the intima ($13.21 \pm 0.84 \mu\text{m}$) and media (234.86

$\pm 13.84 \mu\text{m}$) around the anastomosis site compared to the control group (intima: $17.06 \pm 0.96 \mu\text{m}$; media: $279.88 \pm 34.22 \mu\text{m}$), indicating a statistically significant difference. Additionally, there was an increased intravascular inducible Nitric Oxide Synthase (iNOS) expression in both groups, with a higher percentage in the adhesive group (82.5 % vs. 47.5 %). These results suggest that 2-octylcyanoacrylate adhesive can effectively inhibit stenosis in vascular anastomoses [95]. Although this may seem promising, the inherent cytotoxicity of cyanoacrylate poses boundaries for adoption for intrabody use and requires further extensive testing and characterization [113].

3.5.2. Fibrin glue

Fibrin glue is a topical biological adhesive composed of human fibrinogen, bovine thrombin, and calcium chloride. The latter two components activate human fibrinogen, initiating clot formation and providing tissue adhesion. The glue is completely absorbed during the process [114–116]. Fibrin glue is recognized as a useful hemostatic agent and supplement with other anastomosis techniques. It is important to note that the fibrin glue alone does not have adequate tensile strength to support a successful anastomosis. Therefore, it is used solely as a supplemental adhesive. When used as an adjunct, it has been found to reduce bleeding time, substantially increase tensile strength, and decrease the number of required sutures [98–100]. Recently, Hanneur et al. evaluated its effectiveness in end-to-end arterial microvascular anastomosis using minimal sutures. In their study involving eight anastomoses on seven male rats across different arteries, including femoral, iliac, carotid, and subrenal aorta, the augmented anastomoses with fibrin glue proved significantly quicker (by $10.7 \pm 3.2 \text{ min}$), resulted in less blood loss ($1.3 \pm 0.9 \text{ g}$), and achieved higher quality scores (2.6 ± 2.5 points more) than the conventional technique. Patency rates were similar across both techniques, but notably, three out of seven

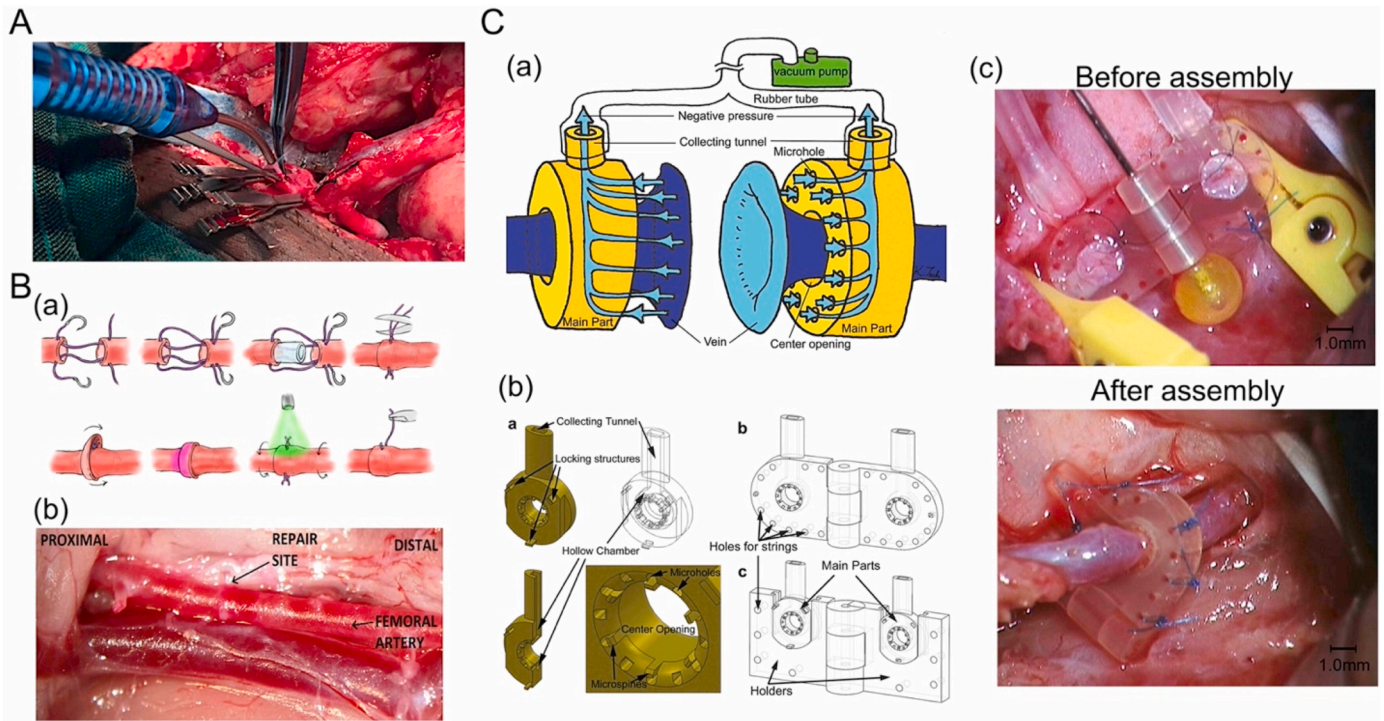


Fig. 10. Assisted approaches for sutureless vascular anastomosis. (A) Laser welding of a vessel. (B) Photochemical tissue bonding around an intraluminal stent, including (a) a schematic showing the stepwise procedure for light-activated anastomosis over a hollow PVA stent, and (b) a close-up photograph of an anastomosed femoral artery immediately after repair using photochemical tissue bonding. (C) Vacuum-assisted microvascular coupler (VaMAC). (a) A schematic of the microvascular ring coupling device that utilizes vacuum negative pressure. (b) Detailed design of the VaMAC from different angles highlighting the collecting tunnel's connection to the hollow chamber and microholes, with enlarged views of the center opening, microholes, and microspines, along with a cross-sectional view showing the tunnel's path to each microhole. Labels b for integrated type and c for disassemble type are provided. (c) Displays from the operating microscope show the vein edges everted and attached to the device by negative pressure before assembly (top) and restored blood flow post-assembly (bottom). Figure is reproduced with minor adaptations from Refs. [54,56,86] with permission.

augmented anastomoses in the femoral subgroup were non-permeable [100].

3.5.3. BioGlue

BioGlue, approved by the FDA in the late 1990s, is tailored for cardiovascular surgeries. Formulated from bovine serum albumin and

glutaraldehyde, it offers a strong bond ideal for vascular applications, resilient to blood pressure variations. Its efficacy, compatibility, and ease of use have established its prominence in cardiovascular settings [101]. However, it has its downsides, including potential immune reactions, disease risk from its bovine origin, non-degradability, and a higher cost [102,103]. In a comparative study between BioGlue and

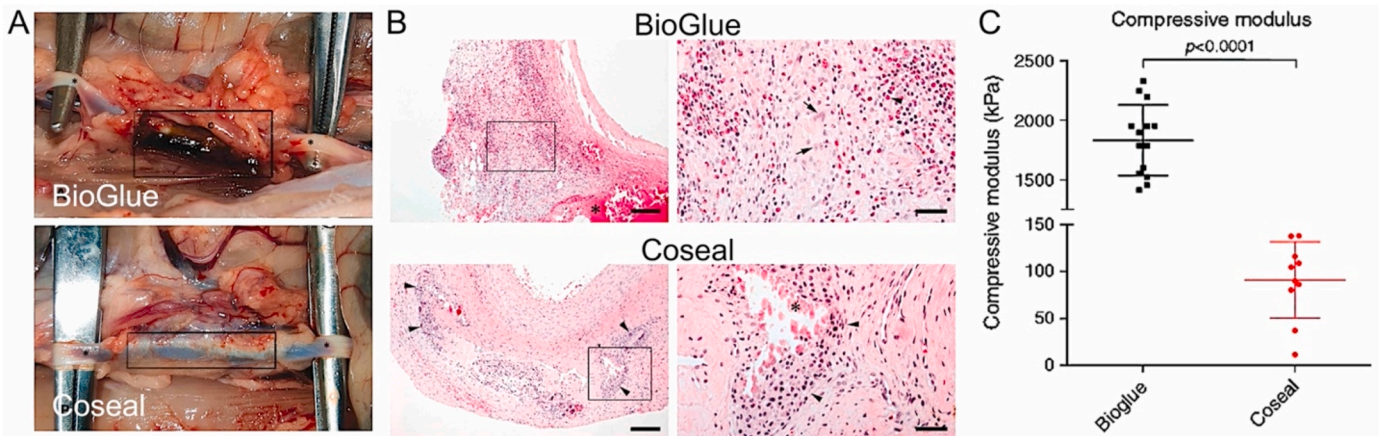


Fig. 11. BioGlue and Coseal application. (A) Representative images of the application sites after 2 weeks: (a) BioGlue, *aorta, grey box: area of application and tissue reaction; (b) Coseal, *aorta, grey box: area of application and tissue reaction%; (c) opened tissue capsule that surrounded the BioGlue residue. (B) Top row: BioGlue. Intense granulomatous inflammation, scale bar = 150 μm, material residues are marked with *; Note lymphocytes, plasma cells, multinucleated giant cells (arrows) and many intensively eosinophilic-stained granulocytes (arrowheads), scale bar = 40 μm. Bottom row: Coseal. Moderate granulomatous inflammation (arrowheads), scale bar = 150 μm; note the presence of many macrophages (arrowheads) and few lymphocytes, scale bar = 40 μm. Localization of high magnification images are highlighted in the low-power images. (C) Comparison of compressive moduli for sealant samples showing mean (central line), SD (bars) and individual sample values (squares/dots). Figure is reproduced with minor adaptations from Ref. [104] with permission.

Coseal (a sealant made from crosslinking PEG chains) in a rabbit aorta suture hole model, the latter showcased some advantages (Fig. 11). The results indicated a significantly less severe inflammatory response to Coseal compared to BioGlue, as evidenced by the histopathological assessment scores (1.56 ± 0.53 for Coseal vs. 2.67 ± 0.50 for BioGlue). Although both materials induced a typical foreign body reaction characterized by granulomatous inflammation, BioGlue also triggered eosinophilic cell infiltration and a higher prevalence of lymphocytes, plasma cells, and B cells. Notably, while Coseal residues were minimal or absent, significant BioGlue deposits remained in the tissue two weeks post-application. Coseal was much more elastic than BioGlue, with a compressive modulus an order of magnitude lower (91 ± 41 vs. 1833 ± 297 kPa). Compared to BioGlue, Coseal elicited a less pronounced inflammatory response in the aortic and peri-aortic tissue in this model and demonstrated greater elasticity [104].

3.5.4. Polyethylene glycol-based adhesives

PEG-based hydrogels are gaining traction as potential tissue adhesives due to their rapid sealing ability and proven biocompatibility (Fig. 11) [104,105]. PEG-based tissue adhesives were initially developed using PEG-containing macromers, extended with poly (α -hydroxy acids), and terminated with acrylate groups. These macromers were photopolymerized directly on tissues without local toxicity to form hydrogel adhesives, adhering through the formation of interpenetrating networks. These adhesives can be tailored to degrade at controlled rates, providing temporary support during the body's natural recovery. Their attributes suggest promise for vascular anastomosis as efficient vessel connectors. However, there is a need to delve into their long-term effectiveness and possible drawbacks. Some challenges include their potential lesser adhesive strength compared to alternatives like cyanoacrylates or BioGlue and ensuring a reliable bond in the body's moist environment. A study involving 40 landrace pigs aimed to evaluate of hemostasis efficacy of four sealants (TachoSil: Fibrin-based collagen sponge; Tisseel: Fibrinogen and thrombin; Coseal: PEG hydrogel-based sealant; and FloSeal: Bovine-derived gelatin granules and human thrombin) in vascular anastomosis. Results showed that after portal vein anastomosis, all sealants achieved better hemostasis than the control, with Coseal being the fastest and FloSeal the slowest. Except for Tisseel, the sealants achieved complete hemostasis and reduced blood loss in aortotomy procedures. This study accentuates the importance of choosing a sealant tailored to the specific surgical environment [117].

3.5.5. Polyurethane-based adhesives

A novel biodegradable polyurethane-based adhesive, VIVO, was introduced as an additional safety measure in surgical procedures [106–108]. Comprising an isocyanate-functionalized prepolymer and an amino-based curing agent, VIVO exhibited impressive adhesive strength on wet tissues. In a study evaluating the efficiency of the VIVO adhesive in microvascular anastomoses, the adhesive was applied to the carotid artery of 60 male rats. Two application methods were tested: a temporary catheter and a custom-shaped memory stent, compared to a suture-only control. Results revealed no occlusion up to 28 days post-surgery for all methods (Fig. 12). The catheter method using VIVO was 32 % faster in anastomosis time and had a similar reduction in bleeding time as the stent method when compared to the control. However, the stent method showed minor stenosis and thrombus formation related to the stent [43,106]. In an *ex vivo* study using chicken femoral arteries, a new polyurethane-based adhesive was compared with fibrin glue and cyanoacrylate for sutureless microsurgical anastomosis. Polyurethane-based adhesive and cyanoacrylate proved significantly faster and more stable than fibrin glue, with both withstanding higher pressures and tensile forces. However, before clinical application of VIVO, further research is needed to optimize its properties for sutureless arterial anastomoses, understand its long-term degradation, and assess its overall safety and effectiveness, particularly in relation to vessel wall stability post-degradation [108,118,119].

3.5.6. Polysaccharide-based adhesives

3.5.6.1. Alginate/polyacrylamide-based adhesive. Polysaccharide adhesives, known for their biocompatibility, safety, and biodegradability, have emerged as a significant component in the field of medical adhesives, although they often require modifications to enhance solubility [109–111]. Recently, Liu et al. developed a durable, biocompatible, bioabsorbable adhesive, marking the first instance of successful main vessel anastomosis in organ transplantation (Fig. 13) [111]. The bioabsorbable hydrogel consists of two crosslinked polymer networks: a calcium ion-crosslinked alginate network and a disulfide-crosslinked polyacrylamide network. The bioconjugation glue is an aqueous mixture of chitosan, EDC [1-(3-Dimethylaminopropyl)-3-ethylcarbodiimide hydrochloride], and NHS (*N*-Hydroxysuccinimide). For adhesion, the glue is applied between the hydrogel and tissue, where EDC and NHS facilitate a reaction between amine groups in chitosan and the carboxyl

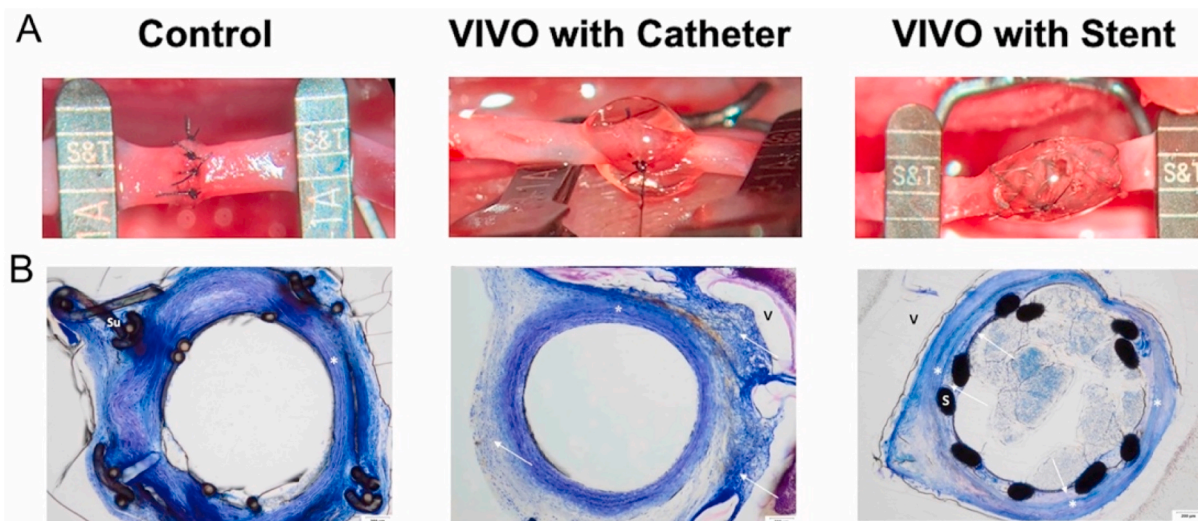


Fig. 12. Long-term outcomes of vascular anastomosis using polyurethane adhesive and shape-memory stent in a rat carotid artery model. (A) Comparative visuals and diagrams of anastomotic methods: traditional suturing, VIVO-assisted anastomosis with temporary catheter and fewer sutures, and VIVO-assisted anastomosis using a shape memory stent with reduced sutures. (B) Toluidine-stained histological sections of microvascular anastomoses at 28 days post-operation, highlighting stent-associated stenosis (indicated by arrows) and media (*). Figure is reproduced with minor adaptations from Ref. [106] with permission.

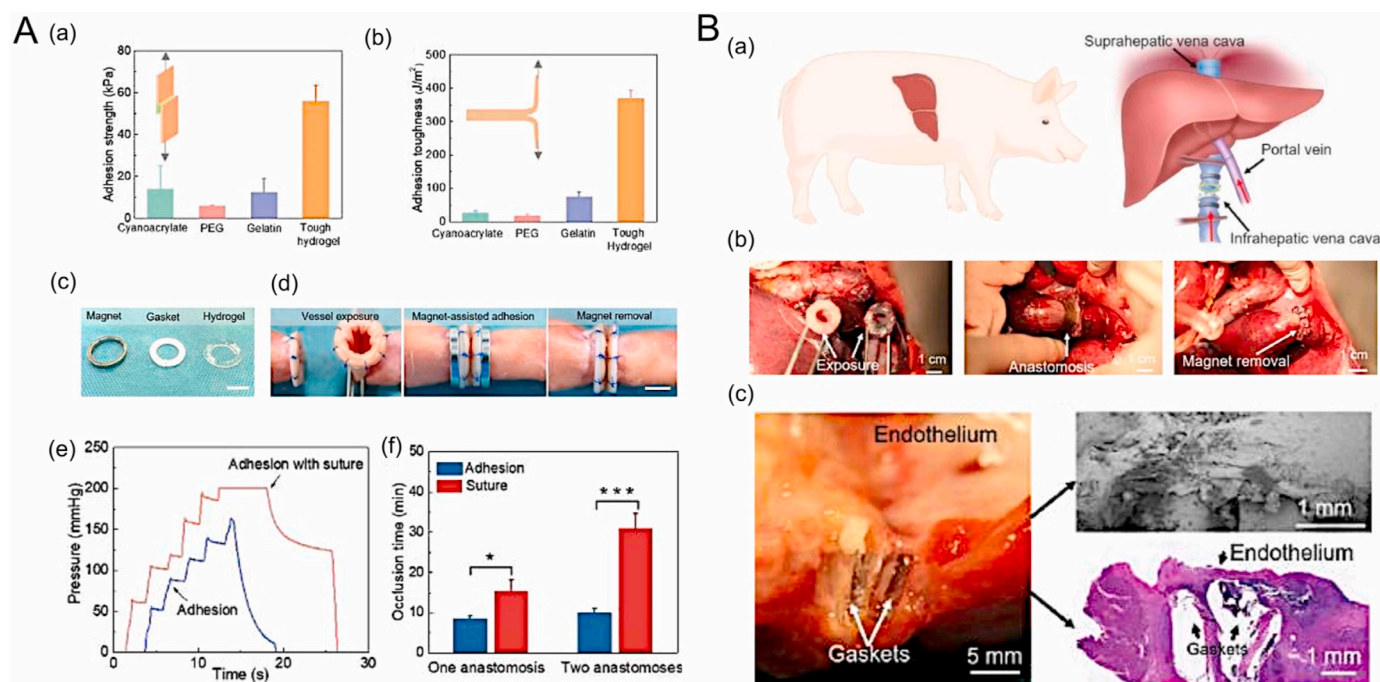


Fig. 13. Adhesive anastomosis in organ transplantation. (A) Demonstration of necessary adhesive property for vascular bonding. (a) Adhesive strength and (b) toughness on porcine aortas. (c) Magnet, gasket, and hydrogel setup for anastomosis. (d) Magnet-assisted anastomosis steps. (e) The adhered vessel can endure an air pressure ~ 160 mm Hg without suture, and ~ 200 mm Hg with sparse sutures. (f) Comparison of the occlusion time for adhesive anastomosis and conventional sutured anastomosis. In connecting two vessel ends, one anastomosis is operated. In transplanting a vessel graft, two anastomoses are operated. (B) Pig liver transplant model via magnet-assisted adhesive anastomosis (a). (b) Donor liver magnet-assisted adhesive anastomosis process. (c) A longitudinal section of the two gaskets. Images of the scanning electron microscopy and hematoxylin-eosin staining. Figure is reproduced with minor adaptations from Ref. [111] with permission.

groups in alginate and tissue [120,121]. Degradation of the adhesive occurs as environmental sodium ions displace calcium in the alginate, and cysteine interacts with the disulfide in the polyacrylamide [122]. They first evaluated the efficacy of various commercial tissue adhesives versus this hydrogel adhesive, utilizing lap shear and peel tests for comparison. Cyanoacrylate adhesive, when applied to a vessel's endothelium and compressed against another vessel for about 10 min, forms a rigid polymer barrier that can obstruct the healing process due to its stiffness and ineffective tissue bonding. Similarly, PEG glue and a gelatin-based adhesive, prepared by dissolving gelatin powder (40 wt%) in hot deionized water (90 °C) with the addition of 0.1 wt% EDC and NHS, exhibit low adhesion strength and toughness. These limitations are primarily due to cyanoacrylate's rapid polymerization on wet aorta surfaces, which prevents proper tissue integration, and the intrinsic material weaknesses of PEG and gelatin. In contrast, this tough hydrogel adhesive demonstrates significantly superior adhesion strength (56 ± 8 kPa) and toughness (368 ± 26 J/m²), with its hysteresis contributing positively to these properties. They further employed magnets, gaskets, and the hydrogel adhesive to create the anastomosis. They found that vessels bonded with this method could withstand air pressures of approximately 160 mm Hg without sutures and up to 200 mm Hg when supported by sparse sutures. The team also showcased the efficacy of this magnet-assisted adhesive anastomosis in pig liver transplants, achieving significantly shorter anastomosis times than traditional suturing methods. The adhesive facilitated vein anastomosis during the surgical procedure and was subsequently absorbed, with the pigs surviving beyond one month. While this technique is still in the early phase, it holds potential for reducing occlusion times in liver transplants and potentially applying to other organ transplants.

3.5.6.2. Alginate/dextran-based adhesives. A novel tissue adhesive, composed of oxidized alginate, oxidized dextran, and polyamidoamine (PAMAM) dendrimer amine, has been developed [123]. The design of

this adhesive utilizes aldehyde groups in the oxidized components to form reversible covalent bonds with tissue amines, while the carboxylic acid groups in oxidized alginate provide additional interactions with both the tissue surface and the PAMAM dendrimer, facilitating strong electrostatic and covalent bonds for improved adhesion. Engineered for practicality, this material can be sprayed and instantly crosslinked *in situ*, making it apt for intricate surgical procedures and complex anatomical structures. In a comprehensive series of *in vivo* tests that adhered to FDA guidelines for medical devices, this hydrogel was benchmarked against Tisseel, known for high biocompatibility but low tissue-adhesion strength, and BioGlue, known for its strong adhesion but lower biocompatibility. The hydrogel formulation demonstrated an optimal balance of adhesion strength and biocompatibility, outperforming these established products in certain respects. Notably, it withstood suprphysiological pressures (around 300 mmHg), proving its efficacy in preventing bleeding in challenging surgical models like rabbit aortic puncture and pig carotid bilateral poly (tetrafluoroethylene) grafts. This material not only exceeded the performance of products like Tisseel and BioGlue but also showed promise for enhancing outcomes in complex vascular surgeries, particularly at challenging tissue-graft interfaces (Fig. 14) [124].

3.5.6.3. Chitosan-based adhesives. Wu et al. have developed a set of flexible and transparent films, chitosan-gallol (CHI-G) and chitosan-boronic acid (CHI-B), to enable a "less-suture" approach to blood vessel anastomosis. The CHI-G film exhibits self-wrapping and sealing capabilities, effectively preventing leakage. In synergy, CHI-B enhances this system by adding mechanical strength through wet fusion with CHI-G. Tested on rat arteries (diameter: 0.64 mm), this method reduced the required stitches from ten to four, saving 27 min per vessel and reducing fibrosis-mediated wall-thickening. This practical less-suture approach offers an efficient and dependable solution, particularly beneficial for anastomosis of multiple vessels in emergencies or small-diameter vessels

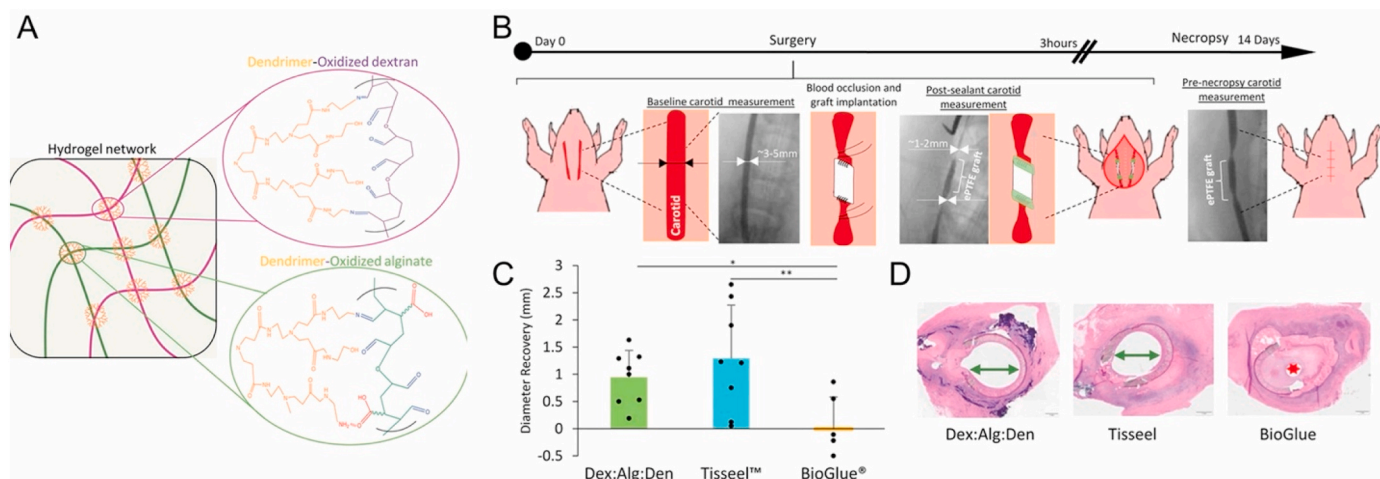


Fig. 14. Evaluation of sprayable hydrogel for vascular anastomosis sealing. (A) Hydrogel network schematic interactions. (B) Bilateral carotid vascular graft and hydrogel in porcine model. (C) Vessel diameter measurement at necropsy, comparing 15%Dex:5%Alg:30%Den, Tisseel, and BioGlue. (D) H&E staining at day 14, showing lumen status for each material (indicated by green arrows or red star); scale bar: 1 mm. Figure is reproduced with minor adaptations from Ref. [124] with permission.

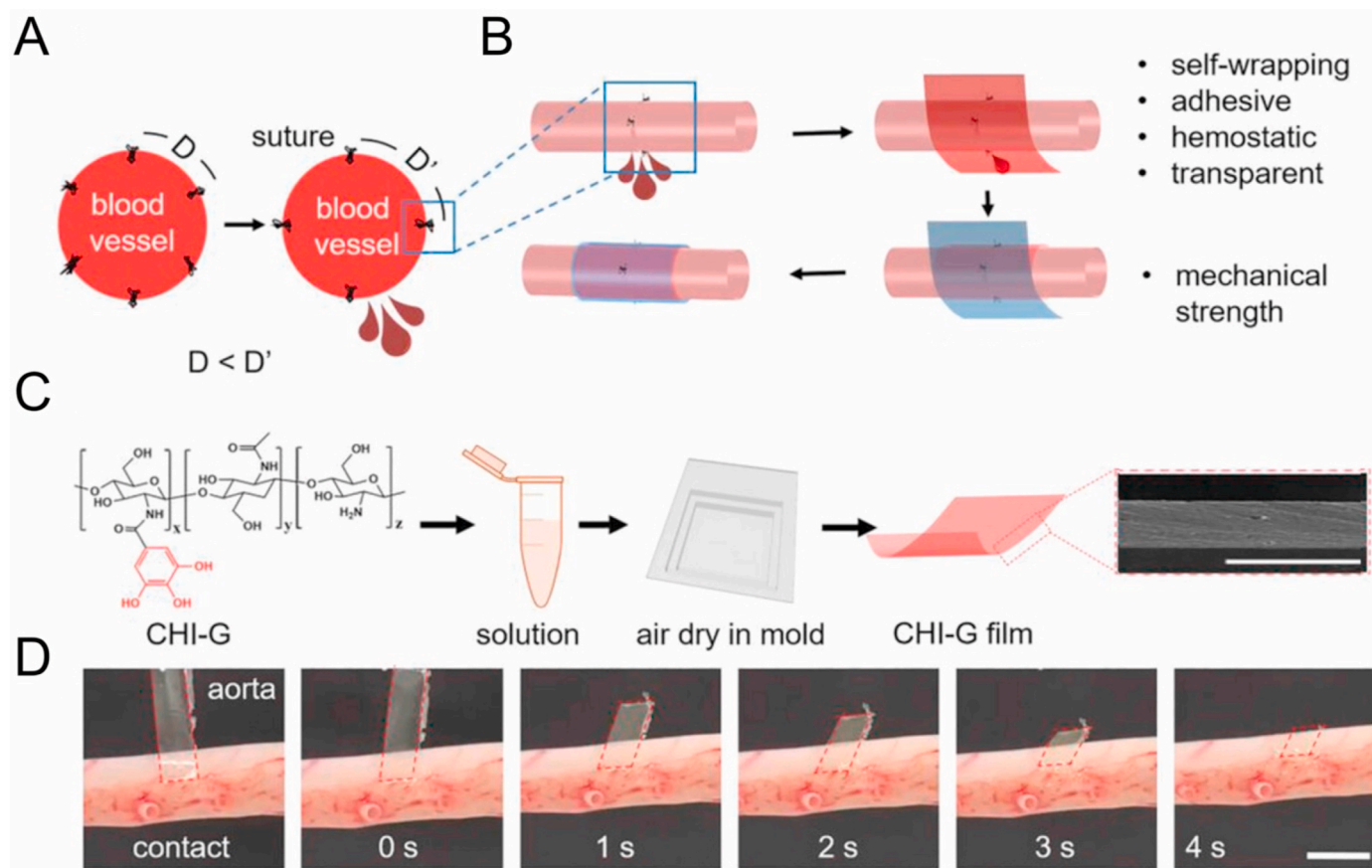


Fig. 15. Less-suture vascular anastomosis with multifunctional biomaterials. (A) Schematic illustrating the risk of bleeding from increased stitch-to-stitch distance (D') compared to typical suture spacing (D) in less-suture scenarios. (B) Demonstration of how wrapping the anastomosis site with CHI-G (red) and CHI-B (blue) films effectively prevents bleeding, even with wider stitch spacing. (C) CHI-G film preparation process involving casting into a mold and air-drying. CHI-G film thickness as determined by SEM. Scale bar: 25 μ m. (D) CHI-G film's self-wrapping capability shown on a porcine aorta; scale bar: 2 cm. Figure is reproduced with minor adaptations from Ref. [125] with permission.

(Fig. 15) [125–127]. Importantly, Chitosan may function in a sutureless technique, rather than less suture, but this requires further study and examination. The long-term safety and efficacy of these hydrogels remain essential areas for evaluation.

3.5.6.4. *Hyaluronic acid-based adhesives.* Hyaluronic acid (HA)-based adhesives are versatile in medical applications, offering benefits like enhanced wound healing and tissue repair [110,128]. Recently, Ren et al. have developed a self-healing, injectable hydrogel adhesive based

on HA. This hydrogel is created by a catalyst-free condensation reaction between *o*-phthalaldehyde (OPA) and *N*-nucleophiles. This involves mixing hydrazide-modified HA with OPA-terminated PEG, forming HA/PEG hybrid hydrogels *in situ* with hydrazone linkages (Fig. 16A). Notably, their formation does not require initiators, catalysts, additives,

or ultraviolet irradiation, and water is the only by-product. These hydrogels adhere strongly to tissues, a result of the spontaneous reaction between OPA and tissue amines (Fig. 16B). Their degradation rate in the body is adjustable by incorporating disulfide bonds in the hydrogel network, which break down in response to thiol-containing compounds

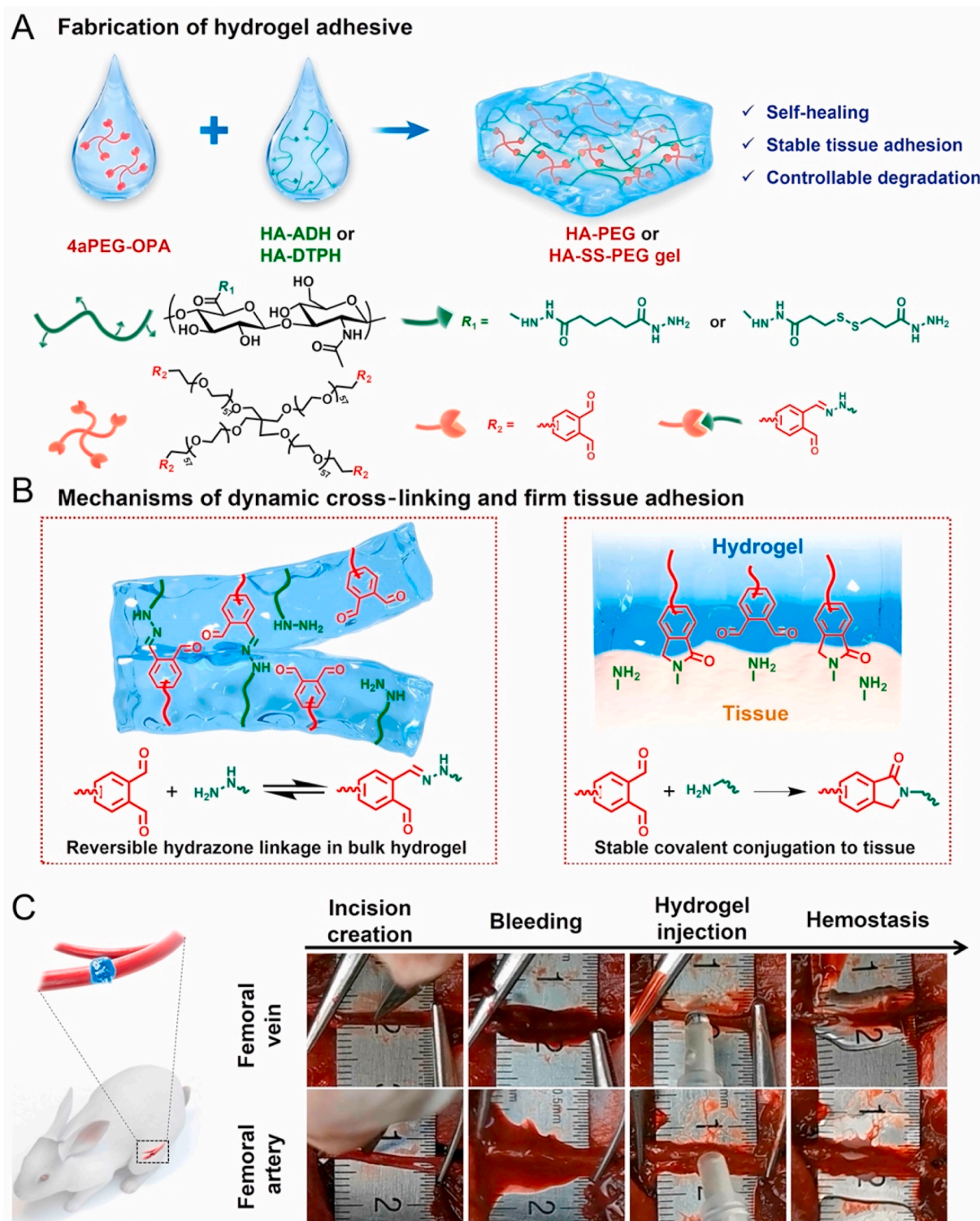


Fig. 16. Schematic illustration of the fabrication, cross-linking/adhesion mechanisms, and applications of HA hydrogel adhesive. (A) Hydrogel adhesive fabrication process, involving the combination of HA-ADH or HA-DTPH with 4aPEG-OPA. (B) Detailed depiction of the dynamic cross-linking mechanisms within the bulk hydrogel and the adhesive interactions between the hydrogel and tissue. (C) Demonstrations of the hydrogel adhesive in medical applications, specifically for hemostasis and skin wound closure. This includes schematic representations and real images showing the effectiveness of a 7 % (w/v) HA-PEG hydrogel in sealing incisions in rabbit femoral veins and arteries. Figure is reproduced with minor adaptations from Ref. [129] with permission.

like glutathione found in the body. The degradation period can be tailored from 6 to 22 weeks by altering the disulfide bond content. These hydrogels have shown superior performance in sealing wounds and promoting healing compared to commercial fibrin and cyanoacrylate glues. This indicates their potential for sutureless wound closure, hemostasis, and leakage prevention in surgical procedures (Fig. 16C) [129, 130]. Despite these advances, the long-term biocompatibility and safety of these hydrogels, especially when used in clinical settings, remain to be fully assessed.

4. Key factors influencing the success of sutureless anastomotic devices

The suture-based anastomosis technique boasts a very high success rate, setting a challenging benchmark for alternative vascular anastomosis methods to meet. Initially, sutured venous anastomoses also achieved high success, but the GEM coupler has become the preferred method for venous anastomosis due to its simplicity and speed, allowing surgeons to complete procedures efficiently with complication rates comparable to those of sutured methods. This suggests a potential preference among surgeons for an arterial anastomotic coupler that offers the effectiveness of hand-sewn techniques but with easier and faster application [14]. Sutured anastomosis typically enjoys success rates above 90 %, with Gerressen et al. reporting a 92 % success rate in sutured microvascular anastomosis across over 400 patients [131]. Similarly, sutureless microvascular anastomosis also reports success rates above 90 %, often compared directly with sutured controls [14]. However, sutured anastomosis has a significant drawback: the ischemic time, which has been repeatedly linked to higher complication rates in free flap transfers [132,133]. Sutureless microvascular anastomosis addresses this issue by significantly reducing ischemic time, potentially reducing related complications [20].

4.1. Device design associated with intimal hyperplasia and thrombogenesis

As seen from the previous devices, a successful arterial sutureless anastomotic device must not require vessel eversion. Currently, technologies that do not require eversion have an intraluminal component, either stent, scaffold, or coupler. For these devices to be successful, they must limit intimal hyperplasia and thrombosis. These complications are often precipitated by the introduction of foreign materials into the bloodstream, which can induce shear stress and trigger inflammatory responses. The endothelium, the innermost lining of blood vessels, plays a crucial role in maintaining a non-thrombogenic environment and regulating vascular tone. However, any disruption to this protective layer, as caused by foreign-body anastomotic devices, can result in endothelial dysfunction. This dysfunction can lead to a series of vascular reactions including vasoconstriction, platelet aggregation, and fibrin clot formation, exacerbated by the upregulation of inflammatory cells [16,134].

The foreign-body response by the anastomotic device is characterized by the release of cytokines and chemokines and the production of growth factors such as platelet-derived growth factor (PDGF), transforming growth factor beta 1 (TGF β 1), and fibroblast growth factor (FGF). These factors stimulate vascular smooth muscle cells in the media layer of vessel to migrate towards the intima. They proliferate in the space between the endothelial lining and the internal elastic lamina. This proliferation, coupled with matrix deposition, leads to intimal thickening, vascular stenosis, and altered blood flow [135]. For example, a near-linear relationship has been established between the degree of stent-induced endothelial cell injury and the severity of intimal hyperplasia [136].

Damage to the blood vessel intima caused by a sutureless anastomotic device can lead to thrombosis. Various anastomotic devices necessitate extensive manipulation; some must be loaded onto a free-

transfer sheet, while others require physical crimping with forceps for successful deployment into a blood vessel [137]. Incorrect deployment of these devices can harm the endothelial cell layer, causing endothelial cells to cease expressing protective factors, such as prostacyclin, nitric oxide, and ecto-adenosine diphosphatase. This damage also diminishes the production of tissue plasminogen activator, which is essential for fibrinolysis and maintaining antithrombotic properties [138]. Moreover, when subendothelial collagen or tissue factors are exposed to circulating platelets, it can trigger a coagulation cascade. This process leads to increased platelet aggregation and fibrin deposition [15]. Activated platelets and injured endothelial cells are crucial in thrombus formation [139]. It is worth noting that thrombosis and inflammation are interconnected. Inflammation can initiate thrombosis, and thrombosis can amplify inflammation [139]. For example, inflammatory molecules such as C-reactive protein can enhance thrombosis by considerably increasing the tissue factor procoagulant activity in monocytes and the levels of von Willebrand factor and plasminogen activator inhibitor-1 [140,141]. To ensure the successful clinical application of sutureless devices, it is vital to optimize their use in blood vessels. This optimization aims to minimize foreign body responses and reduce intimal damage, thereby preventing complications such as intimal hyperplasia and thrombosis.

4.2. Device design on blood flow dynamics and thrombogenesis

As previously described, intraluminal devices can be used for sutureless arterial anastomosis without eversion. Another factor predisposing to thrombosis is changes in blood flow along the endothelium. Understanding blood flow dynamics is crucial in the development of intraluminal sutureless anastomotic devices [142,143]. Wall shear stress (WSS), the frictional force exerted by blood flow on the endothelial surface, is a key parameter in these dynamics. Turbulent flow, characterized by blood not flowing parallel to the vessel, leads to low WSS. This low WSS stimulates endothelial cell proliferation and the secretion of prothrombotic and vasoconstrictive substances [144]. In environments with low WSS, the weaker blood flow force fails to prevent cell-cell interactions, platelet adhesions, and interactions with leukocytes and erythrocytes [145]. Vascular cells in low WSS conditions upregulate atherogenic genes, triggering vascular remodeling and increased thrombin generation [146]. While high WSS is generally beneficial, problems arise when it exceeds 5 Pa for extended periods, leading to platelet activation and thrombosis. Under such conditions, prothrombotic factors are upregulated, and platelets are more prone to pathologic binding and thrombosis due to their proximity to the vessel wall [145].

In terms of intraluminal stent, there are four main design components that can affect blood flow dynamics: strut thickness, design, deployment, and material. Saito et al. underwent a meta-analysis of first and second-generation drug-eluting stents and demonstrated that thinner struts (60–140 μ m) were associated with lower rates of stent thrombosis within a year, likely due to decreased blood recirculation, turbulent flow, and thrombus formation area (Fig. 17) [147–149]. Mejia et al. found that elliptical and teardrop stent designs resulted in lower WSS peaks at strut impact and higher WSS between struts compared to circular and square designs. These patterns of WSS reduce thrombosis and stenosis potential [150,151]. In terms of stent deployment, mispositioning the stent causes increased turbulent flow and recirculation, leading to a significant rise in thrombogenicity biomarkers [152]. Lastly, Han et al. investigated the effects of low and high WSS on the thrombogenicity of different materials: acrylic, stainless steel, zirconia ceramic, polyvinyl chloride (PVC), silicone, Dacron, and PTFE. They found that at high WSS, stainless steel and PTFE were the most thrombogenic, whereas acrylic, silicone, and PVC were not. In contrast, at low WSS, stainless steel and PTFE were least thrombogenic, and PVC, silicone, and acrylic were most thrombogenic [153]. Therefore, the optimal selection of an anastomotic stent requires careful consideration of

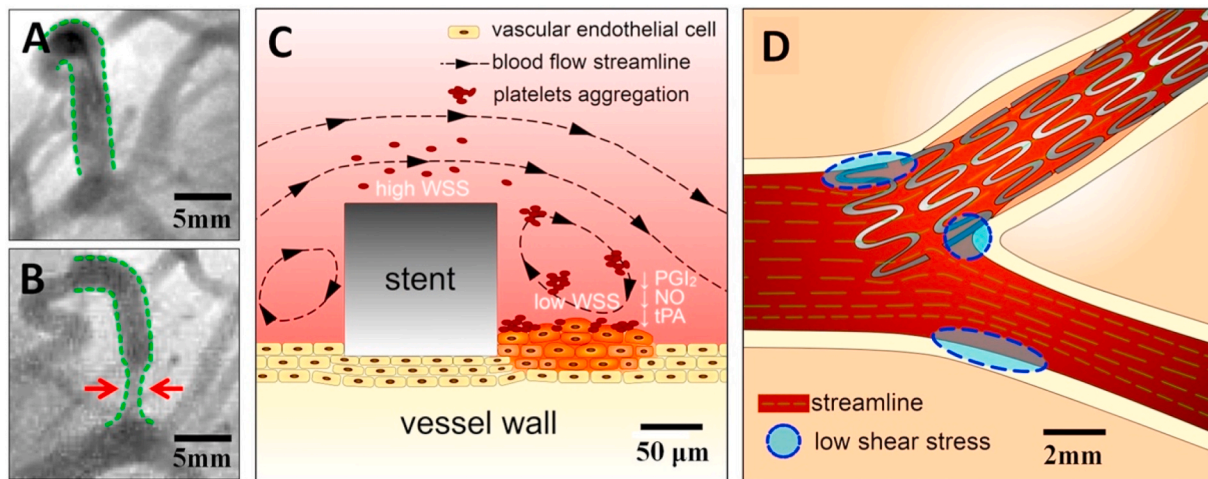


Fig. 17. Analysis of stent-related complications post-PCI. (A) Angiography image illustrating a stented branch vessel immediately after percutaneous coronary intervention (PCI), showing stent expansion. (B) Evidence of restenosis at the stent site one year post-PCI, highlighted by red arrows. (C) Illustration explaining stent thrombogenicity: stent thickness leads to high wall shear stress (WSS) over the stent and low wall shear stress at stent-vessel interface, promoting epithelial cell outgrowth and subsequent restenosis. (D) Impact of stent positioning on WSS and potential restenosis sites, with blue regions indicating areas susceptible to restenosis due to stent placement. Figure is reproduced with minor adaptations from Ref. [149] with permission.

design, deployment, and material to minimize complications and failures.

5. FDA approval process for vascular anastomotic approaches

Sutureless anastomotic devices, like all medical devices, are subject to stringent FDA regulations and multiple testing phases prior to approval. The approval process typically involves three key phases. Phase one is centered around the creation and laboratory testing of the device. Phase two involves *in vivo* testing using animal models, primarily to assess safety. The third phase encompasses clinical trials on human subjects, aimed at evaluating both the safety and efficacy of the device. Following successful trials, the final step is obtaining market approval from the FDA [154]. Sutureless anastomotic devices are categorized as class III, which is subject to the highest level of regulation. This is due to their vital function and potential risks. Class III devices require premarket approval (PMA), demanding extensive preclinical and clinical data to ensure safety and effectiveness. It is also noteworthy that after initial approval, any device modifications may be approved through the less rigorous 510(k) clearance, if the modified device is similar to an existing approved device, allowing efficient updates without compromising safety and efficacy [155].

Tissue adhesives, often implanted for long durations and biodegradable, are classified as high-risk (Class III) devices by the FDA, facing tough regulatory challenges. Although the 510(k) process offers a simplified route for similar devices, new bioadhesives typically undergo the PMA process, necessitating in-depth safety and efficacy evaluations. This demanding process can pose significant barriers to market entry, given its associated risks, high costs, and protracted timelines [112].

6. Potential impacts of advanced sutureless vascular anastomosis

Sutureless anastomosis is highly sought after in healthcare systems, as it could significantly reduce surgical time, skill requirements, and resources compared to hand-sewn anastomosis [156,157]. Modern microsurgery training can be resource-intensive and inconsistent, with a significant number of programs lacking formal curriculums and diverse anastomosis models [158]. A sutureless anastomotic device will promote easy ligation and adherence and will be feasible for all surgeons, not just specially trained microsurgeons. This impact is crucial in third world countries where there are resource constraints and a shortage of

plastic surgeons [159,160]. With surgical conditions accounting for 11 % of global disability-adjusted life years lost, the potential to broaden access to microsurgery through a sutureless anastomotic device could be transformative [161].

The second potential benefit of a sutureless microvascular anastomotic device may potentially decrease post-surgical complication rates. Even with the myriad of resources in the US, the intricacy and complexity of microvascular surgery promotes many complications. Complications in microvascular surgery, such as intraoperative flap failure and fat necrosis, can be associated with numerous factors like inexperienced surgeons, the presence of junior residents, and longer operating times. These complications often lead to longer hospital stays and higher costs [132,162]. Similar issues are seen in other medical fields where microsurgery is essential, like orthopedics, where ischemic time over 2 h can lead to severe complications including amputation [163]. With a sutureless device, flap ischemic time, and total operative time could be significantly reduced, resulting in less complications associated with necrosis. Additionally, a sutureless device will also promote easier anastomosis for less experienced surgeons, further reducing complications (Fig. 18).

A sutureless anastomotic device could also substantially reduce economic and emotional cost for the hospital and patient. Current microvascular anastomosis can lead to longer operative times, higher revision rates, and more post-operative complications. Each of these impacts the patients, potentially necessitating additional surgeries and impacting their mental health. Furthermore, these surgical complications impose a considerable economic burden for both patients and hospitals. With a sutureless device, anastomosis could be conducted much more swiftly, greatly reducing ischemic times and subsequent complications. This could lead to fewer revision surgeries and significant cost savings in microvascular surgeries.

7. Summary and outlook

In our review, we explore the evolution and current state of sutureless anastomosis, highlighting its benefits and the pressing need for devices tailored for microvascular arterial anastomosis. Although the GEM coupler has been effective in venous anastomosis, a similar breakthrough for arterial anastomosis remains elusive. We examine alternative methods like laser or photochemical anastomosis, noting their drawbacks such as potential tissue harm, thrombosis risk, and the challenges they present in less-resourced medical settings. Likewise,

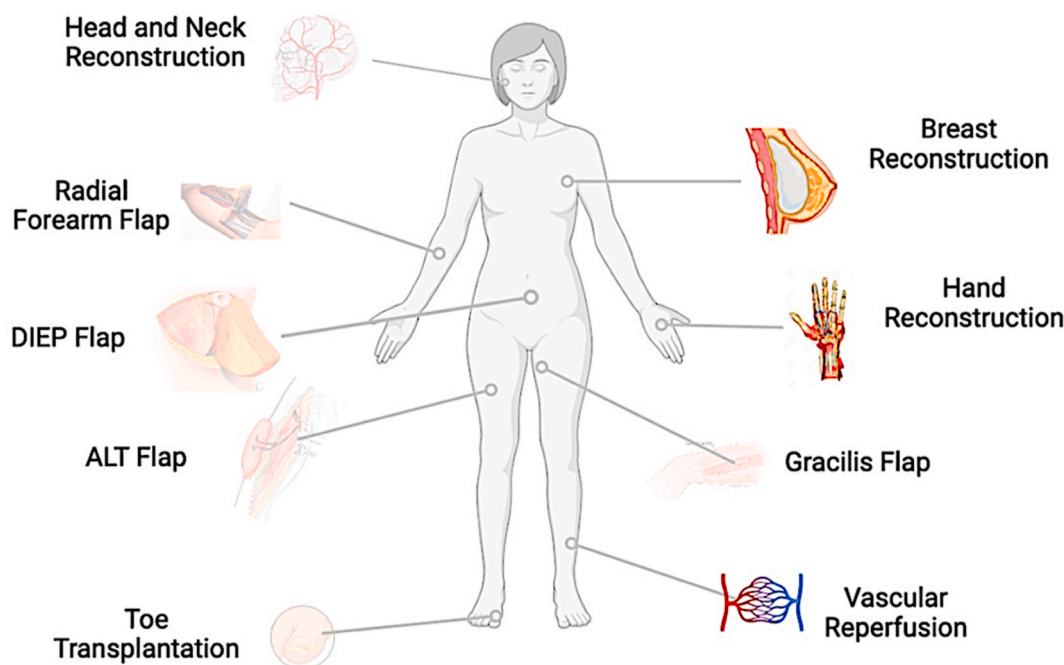


Fig. 18. Potential impacts for sutureless microvascular anastomosis. Each of the procedures shown can require arterial anastomosis. These can all be significantly impacted by a sutureless arterial anastomotic device.

vacuum-assisted anastomosis, despite being innovative, relies heavily on advanced technology and is extraluminal.

Overall, although there are many devices currently being researched, many fail to address the main concern of the GEM coupler–required vessel eversion. For a vascular device to promote sutureless arterial anastomosis, it must not require vessel eversion and it must have feasible implementation. Of the researched devices, the two categories that exhibit these critical properties are intraluminal stents and tissue adhesives. Bioabsorbable stents are particularly notable for offering the benefits of standard intraluminal stents but with less reliance on anticoagulants, facilitating reendothelialization and reducing thrombosis risks. However, these devices are relatively new and require optimization of biodegradable profile and downstream effects. Most studies presented demonstrate proof of concept designs. Non-biodegradable intraluminal stents require drug elution and face difficulty with thrombosis. These stents have potential but again require substantial optimization of specific stent design and drug elution to decrease thrombosis risk. Tissue adhesives, another area of potential, could enable immediate and robust closure while being biocompatible. However, advancements are needed in enhancing adhesive strength, biodegradability, and compatibility with tissue healing. Critical factors affecting thrombogenicity, such as vessel injury, inflammation related to the device, and changes in blood flow, must be considered. Effective sutureless anastomotic devices should be designed to minimize inflammation and promote endothelial repair. Also, both tissue adhesives and intraluminal stents have been studied in small sample animal models. A larger cohort study in a large animal model is required to elucidate the true effectiveness of current devices. Lastly, a large challenge to creating a sutureless arterial anastomotic device is FDA approval. Arterial anastomosis will be a new indication for many devices and will likely need PMA for FDA clearance, requiring large scale clinical trials.

With the progression of material science, we anticipate the emergence of new bioabsorbable polymers and biologics, improving the properties of stents in terms of durability, absorption, and biocompatibility. Concurrent advancements in tissue adhesives are likely to complement these developments, tailoring solutions to diverse surgical requirements. The advent of technologies like 3D printing could enable custom device designs based on individual vascular anatomy, while

breakthroughs in computational modeling are expected to facilitate the optimization of new devices by predicting their behavior before physical creation [164–168]. These developments signal a promising future for sutureless microvascular anastomotic techniques, potentially revolutionizing plastic and reconstructive surgery in the years ahead.

Ethics approval and consent to participate

Not Applicable.

CRediT authorship contribution statement

Joseph G. Ribaldo: Investigation, Writing – original draft, Writing – review & editing. **Kevin He:** Writing – original draft. **Sarah Madira:** Writing – original draft. **Emma R. Young:** Writing – review & editing. **Cameron Martin:** Writing – review & editing. **Tingying Lu:** Writing – review & editing. **Justin M. Sacks:** Conceptualization, Supervision, Writing – review & editing. **Xiaowei Li:** Conceptualization, Supervision, Writing – review & editing.

Declaration of competing interest

The authors declare no competing financial interests.

Acknowledgements

We are thankful for the funding support received from the Institute of Materials Science and Engineering, and the Institute of Clinical and Translational Sciences grant UL1TR002345 from the National Center for Advancing Translational Sciences of the NIH, DoD Peer Reviewed Medical Research Program Discovery Award (HT94252310022 to Li and Sacks), Traumatic Brain Injury and Psychological Health Research Program Idea Development Award (W81XWH-22-1-0785 to Li), and NIH R01HL168513 (Li).

References

- [1] D.P. Mallela, et al., A systematic review of sutureless vascular anastomosis technologies, *Semin. Vasc. Surg.* 34 (2021) 247–259.
- [2] W.R. Moritz, et al., The history and innovations of blood vessel anastomosis, *Bioengineering (Basel)* 9 (2022).
- [3] V. Ilie, R. Haddad, E. Moisisidis, Sutureless microvascular anastomosis: literature review, *Int. Microsurg. J.* 3 (2019).
- [4] E.W. Weiss, C.R. Lam, Tantalum tubes in the non-suture method of blood vessel anastomosis, *Am. J. Surg.* 80 (1950) 452–454.
- [5] A.H. Blakemore, J.W. Lord, A nonsuture method of blood vessel anastomosis: review of experimental study report of clinical cases, *Ann. Surg.* 121 (1945) 435–452.
- [6] C.W. Hughes, W.F. Bowers, Blood vessel surgery, *Am. J. Surg.* 85 (1953) 174–178.
- [7] S. Smith, A soluble rod as an aid to vascular anastomosis: an experimental study, *Arch. Surg.* 41 (1940) 1004–1007.
- [8] O. Swenson, R.E. Gross, Absorbable fibrin tubes for vein anastomoses, *Surgery* 22 (1947) 137–143.
- [9] T. Takaro, A simple stapling device for the anastomosis of blood vessels, *J. Thorac. Cardiovasc. Surg.* 40 (1960) 673–684.
- [10] P.B. Samuels, Method of blood vessel anastomosis by means of metal clips: an experimental study, *A.M.A. Arch. Surg.* 70 (1955) 29–38.
- [11] I.C.D.Y.M. Wolf-de Jonge, J.F. Beek, R. Balm, 25 Years of laser assisted vascular anastomosis (LAVA): what have we learned? *Eur. J. Vasc. Endovasc. Surg.* 27 (2004) 466–476.
- [12] Y. Obora, N. Tamaki, S. Matsumoto, Nonsuture microvascular anastomosis using magnet rings: preliminary report, *Surg. Neurol.* 9 (1978) 117–120.
- [13] J.J. Wozniak, A new sutureless method for the anastomosis of blood vessels, *Biomater. Med. Dev. Artif. Organs* 13 (1985) 51–60.
- [14] H. Umezawa, Y. Hokazono, M. Taga, R. Ogawa, Applying the microvascular anastomotic coupler device to end-to-side venous anastomosis in reconstructive surgery, *Plastic and Reconstructive Surg. – Glob. Open* 10 (2022) e4018.
- [15] N. Saegusa, et al., Sutureless microvascular anastomosis assisted by an expandable shape-memory alloy stent, *PLoS One* 12 (2017) e0181520.
- [16] Y. Jeong, Y. Yao, E.K.F. Yim, Current understanding of intimal hyperplasia and effect of compliance in synthetic small diameter vascular grafts, *Biomater. Sci.* 8 (2020) 4383–4395.
- [17] A.R. Gundale, Y.J. Berkovic, P. Entezami, C.O. Nathan, B.A. Chang, Systematic review of microvascular coupling devices for arterial anastomoses in free tissue transfer, *Laryngoscope Investig. Otolaryngol.* 5 (2020) 683–688.
- [18] S. Cappelletti, et al., Non-invasive estimation of vascular compliance and distensibility in the arm vessels: a novel ultrasound-based protocol, *Quant. Imag. Med. Surg.* 12 (2022) 3515–3527.
- [19] Synovis, GEM Flow Coupler Device System. https://www.synovismicro.com/pdfs/IFUs/Flow_Coupler_Device_IFU_MS-0723404.pdf.
- [20] E.F. O'Connor, et al., The microvascular anastomotic coupler for venous anastomoses in free flap breast reconstruction improves outcomes, *Gland Surg.* 5 (2016) 88–92.
- [21] L.K. Head, D.R. McKay, Economic comparison of hand-sutured and coupler-assisted microvascular anastomoses, *J. Reconstr. Microsurg.* 34 (2018) 71–76.
- [22] R.A.J. Wain, J.P.M. Whitty, W. Ahmed, in: M.J. Jackson, W. Ahmed (Eds.), *Micro and Nanomanufacturing Volume II*, Springer International Publishing, Cham, 2018, pp. 545–559.
- [23] N. Alkhamesi, PAS-port Proximal Anastomosis System, SAGES, 2021.
- [24] W. Kirsch, Applications of the AnastoClip® for neurosurgical interventions, *Techniques in Neurosurg. & Neurol.* 1 (2018).
- [25] A. Ebner, M.D. Ross, M.D. John, Alexander MD. Yevzlin, Minimally invasive sutureless anastomosis of an AV hemodialysis graft, *Endovasc. Today* (2014).
- [26] C.J. Shaw, G.R. ter Haar, I.H. Rivens, D.A. Giussani, C.C. Lees, Pathophysiological mechanisms of high-intensity focused ultrasound-mediated vascular occlusion and relevance to non-invasive fetal surgery, *J. R. Soc. Interface* 11 (2014) 20140029.
- [27] G. Pafitanis, et al., Microvascular anastomotic arterial coupling: a systematic review, *J. Plast. Reconstr. Aesthetic Surg.* 74 (2021) 1286–1302.
- [28] J.D. Puskas, et al., Evaluation of the PAS-Port Proximal Anastomosis System in coronary artery bypass surgery (the EPIC trial), *J. Thorac. Cardiovasc. Surg.* 138 (2009) 125–132.
- [29] LeMaitre, AnastoClip AC Closure System. <https://www.lemaitre.com/products/anastoclip-ac-closure-system>.
- [30] C. Reddy, D. Pennington, H. Stern, Microvascular anastomosis using the vascular closure device in free flap reconstructive surgery: a 13-year experience, *J. Plast. Reconstr. Aesthetic Surg.* 65 (2012) 195–200.
- [31] C.J. Zeebregts, Non-penetrating clips for vascular anastomosis, *Eur. J. Vasc. Endovasc. Surg.* 30 (2005) 288–290.
- [32] J.M. Findlay, J.F. Megyesi, Carotid arteriotomy closure using a vascular clip system, *Neurosurgery* 42 (1998) 550–553. ; discussion 553–554.
- [33] J.M. Donker, M.J. Tijnagel, M.L. van Zeeland, E.J. Veen, L. van der Laan, Anastomoses in the common femoral artery, vascular clips or sutures? A feasibility study, *Ann. Vasc. Surg.* 27 (2013) 194–198.
- [34] A. Ebner, J.R. Ross, C.M. Setum, M.J. Kallok, A.S. Yevzlin, Transcatheter anastomosis connector system for vascular access graft placement: results from a first-in-human pilot study, *J. Vasc. Access* 17 (2016) 111–117.
- [35] J.S. Burgess, et al., Prospective multicenter study of a novel endovascular venous anastomotic procedure and device for implantation of an arteriovenous graft for hemodialysis, *J. Vasc. Access* (2023) 11297298231159691.
- [36] W. Jeong, K. Kim, D. Son, Y. Kim, New absorbable microvascular anastomotic devices representing a modified sleeve technique: evaluation of two types of source material and design, *Sci. Rep.* 9 (2019) 10945.
- [37] S. An, et al., Biocompatibility and patency of a novel titanium vascular anastomotic device in a pig jugular vein, *Sci. Rep.* 11 (2021) 17512.
- [38] K. Ueda, T. Mukai, S. Ichinose, Y. Koyama, K. Takakuda, Bioabsorbable device for small-caliber vessel anastomosis, *Microsurgery* 30 (2010) 494–501.
- [39] H. Li, et al., Vascular coupling system for end-to-end anastomosis: an in vivo pilot case report, *Cardiovasc. Eng. Technol.* 8 (2017) 91–95.
- [40] M. Kapischke, D. Gerhard, A. Pries, Sutureless open vascular anastomosis connector: an experimental study, *Vascular* 25 (2017) 101–104.
- [41] K.G. Chitkara, H. Anthony, Second - versus first-generation drug-eluting stents, *Intervent. Cardiol.* 5 (2010) 23–26, 2010.
- [42] A.V. Finn, et al., Vascular responses to drug eluting stents: importance of delayed healing, *Arterioscler. Thromb. Vasc. Biol.* 27 (2007) 1500–1510.
- [43] M. Heitzer, et al., Microvascular anastomosis techniques using the medical adhesive VIVO and expandable micro-stents in a rat carotid artery model, *Annals of Anatomy - Anatomischer Anzeiger* 238 (2021) 151782.
- [44] D.-H. Kim, et al., Microneedle vascular couplers with heparin-immobilized surface improve suture-free anastomosis performance, *ACS Biomater. Sci. Eng.* 4 (2018) 3848–3853.
- [45] A. Farzin, et al., 3D-Printed sugar-based stents facilitating vascular anastomosis, *Adv. Healthcare Mater.* 7 (2018) e1800702.
- [46] C. García-Mintegui, et al., Zn-Mg and Zn-Cu alloys for stenting applications: from nanoscale mechanical characterization to in vitro degradation and biocompatibility, *Bioact. Mater.* 6 (2021) 4430–4446.
- [47] Y. Li, et al., Biodegradable magnesium alloy stents as a treatment for vein graft restenosis, *Yonsei Med. J.* 60 (2019) 429–439.
- [48] R.R. Jose, et al., Rapid prototyped sutureless anastomosis device from self-curing silk bio-ink, *J. Biomed. Mater. Res. B Appl. Biomater.* 103 (2015) 1333–1343.
- [49] W.J. McCarthy, et al., Vascular anastomoses with laser energy, *J. Vasc. Surg.* 3 (1986) 32–41.
- [50] Z. Mbaidjol, M.H. Stoffel, M. Frenz, M.A. Constantinescu, A novel technique for laser-assisted revascularization: an in vitro pilot study, *Laser Med. Sci.* 36 (2021) 855–862.
- [51] D.L. Abramson, W.W. Shaw, B.R. Kamat, A. Harper, C.R. Rosenberg, Laser-assisted venous anastomosis: a comparison study, *J. Reconstr. Microsurg.* 7 (1991) 199–203.
- [52] F.M. Leclère, V. Duquennoy-Martinet, M. Schoofs, B. Buys, S. Mordon, [Thirty years of laser-assisted microvascular anastomosis (LAMA): what are the clinical perspectives?], *Neurochirurgie* 57 (2011) 1–8.
- [53] H. Xie, S.C. Bendre, A.P. Burke, K.W. Gregory, A.P. Furnary, Laser-assisted vascular end to end anastomosis of elastin heterograft to carotid artery with an albumin stent: a preliminary in vivo study, *Laser Surg. Med.* 35 (2004) 201–205.
- [54] P. Senthil-Kumar, et al., An intraluminal stent facilitates light-activated vascular anastomosis, *J. Trauma Acute Care Surg.* 83 (2017) S43–s49.
- [55] A.C. O'Neill, et al., Microvascular anastomosis using a photochemical tissue bonding technique, *Laser Surg. Med.* 39 (2007) 716–722.
- [56] K. Tachi, K.S. Furukawa, I. Koshima, T. Ushida, New microvascular anastomotic ring-coupling device using negative pressure, *J. Plast. Reconstr. Aesthetic Surg.* 64 (2011) 1187–1193.
- [57] K. Tachi, K.S. Furukawa, I. Koshima, T. Ushida, New microvascular anastomotic device for end-to-side anastomosis using negative pressure; a preliminary study, *J. Plast. Surg. Hand Surg.* 54 (2020) 167–171.
- [58] M. Hoogewerf, J. Schuurkamp, J.C. Kelder, S. Jacobs, P.A. Doevendans, Sutureless versus hand-sewn coronary anastomoses: a systematic review and meta-analysis, *J. Clin. Med.* 11 (2022) 749.
- [59] U. Klima, et al., Magnetic vascular coupling for distal anastomosis in coronary artery bypass grafting: a multicenter trial, *J. Thorac. Cardiovasc. Surg.* 126 (2003) 1568–1574.
- [60] C. Vicol, S. Eifert, M. Oberhoffer, P. Boekstegers, B. Reichart, Mid-term patency after magnetic coupling for distal bypass anastomosis in coronary surgery, *Ann. Thorac. Surg.* 82 (2006) 1452–1456.
- [61] Q. Lu, et al., End-to-end vascular anastomosis using a novel magnetic compression device in rabbits: a preliminary study, *Sci. Rep.* 10 (2020) 5981.
- [62] U. Klima, M. Maringka, E. Bagaev, S. Kirschner, A. Haverich, Total magnetic vascular coupling for arterial revascularization, *J. Thorac. Cardiovasc. Surg.* 127 (2004) 602–603.
- [63] C. Gehrke, H. Li, H. Sant, B. Gale, J. Agarwal, Design, fabrication and testing of a novel vascular coupling device, *Biomed. Microdevices* 16 (2014) 173–180.
- [64] R. Brewster, et al., A biodegradable vascular coupling device for end-to-end anastomosis, *J. Med. Biol. Eng.* 38 (2018) 715–723.
- [65] L. Czuba, Application of plastics in medical devices and equipment, *Handb. Polym. Appl. Med. Med. Devices* 9–19 (2014).
- [66] I.V. Panayotov, V. Orti, F. Cuisinier, J. Yachouh, Polyetheretherketone (PEEK) for medical applications, *J. Mater. Sci. Mater. Med.* 27 (2016) 118.
- [67] K. Miller, J.E. Hsu, L.J. Soslowsky, in: P. Ducheyne (Ed.), *Comprehensive Biomaterials*, Elsevier, Oxford, 2011, pp. 257–279.
- [68] P. Gentile, V. Chiono, I. Carmagnola, P.V. Hatton, An overview of poly(lactic-co-glycolic) acid (PLGA)-based biomaterials for bone tissue engineering, *Int. J. Mol. Sci.* 15 (2014) 3640–3659.
- [69] J.E. Bergsma, et al., In vivo degradation and biocompatibility study of in vitro pre-degraded as-polymerized polylactide particles, *Biomaterials* 16 (1995) 267–274.

- [70] B. Yue, P. Ye, C. Liu, Z. Chang, Application of poly(L, L-lactide-co-ε-caprolactone) copolymer medical implants to the treatment of massive rotator cuff tears in orthopedic shoulder surgery, *AIP Adv.* 10 (2020) 115212.
- [71] U.J. Park, et al., Fabrication of a novel absorbable vascular anastomosis device and testing in a pig liver transplantation model, *Ann. Biomed. Eng.* 47 (2019) 1063–1077.
- [72] D. He, et al., 3D-Printed PEEK extravascular stent in the treatment of nutcracker syndrome: imaging evaluation and short-term clinical outcome, *Front. Bioeng. Biotechnol.* 8 (2020) 732.
- [73] M. Meseeha, M. Attia, in: *StatPearls*, Treasure Island (FL), 2023.
- [74] A. Roguin, Stent: the man and word behind the coronary metal prosthesis, *Circ Cardiovasc. Interv.* 4 (2011) 206–209.
- [75] P.W. Serruys, et al., A comparison of balloon-expandable-stent implantation with balloon angioplasty in patients with coronary artery disease. Benestent Study Group, *N. Engl. J. Med.* 331 (1994) 489–495.
- [76] H. Ullrich, T. Münzel, T. Gori, Coronary stent thrombosis- predictors and prevention, *Dtsch Arztebl. Int.* 117 (2020) 320–326.
- [77] P. Chakraborty Banerjee, S. Al-Saadi, L. Choudhary, S.E. Harandi, R. Singh, Magnesium implants: prospects and challenges, *Materials* 12 (2019).
- [78] J.S. Miller, et al., Rapid casting of patterned vascular networks for perfusable engineered three-dimensional tissues, *Nat. Mater.* 11 (2012) 768–774.
- [79] B.N. Moeun, et al., Improving the 3D printability of sugar glass to engineer sacrificial vascular templates, *3D Print. Addit. Manuf.* 10 (2023) 869–886.
- [80] K.A. Gerling, et al., A novel sutureless anastomotic device in a swine model: a proof of concept study, *J. Surg. Res.* 291 (2023) 116–123.
- [81] R.R. Jose, J.E. Brown, K.E. Polido, F.G. Omenetto, D.L. Kaplan, Polyol-silk bioink formulations as two-Part Room-temperature curable materials for 3D printing, *ACS Biomater. Sci. Eng.* 1 (2015) 780–788.
- [82] S. Lu, et al., Insoluble and flexible silk films containing glycerol, *Biomacromolecules* 11 (2010) 143–150.
- [83] S. Kiritani, et al., Silk fibroin vascular graft: a promising tissue-engineered scaffold material for abdominal venous system replacement, *Sci. Rep.* 10 (2020) 21041.
- [84] A. Alessandrino, et al., Three-layered silk fibroin tubular scaffold for the repair and regeneration of small caliber blood vessels: from design to in vivo pilot tests, *Front. Bioeng. Biotechnol.* 7 (2019) 356.
- [85] K.K. Jain, W. Gorisch, Microvascular repair with neodymium-YAG laser, *Acta Neurochir. Suppl.* 28 (1979) 260–262.
- [86] S. Kumar, et al., Laser-assisted microvascular anastomosis of free flaps in reconstruction of orofacial defects: a comparative study among conventional methods and diode laser anastomosis, *J. Maxillofac. Oral Surg.* 20 (2021) 635–641.
- [87] B.B. Scott, M.A. Randolph, F.P.S. Guastaldi, R.C. Wu, R.W. Redmond, Light-activated vascular anastomosis, *Surg. Innovat.* 30 (2023) 143–149.
- [88] E.I. Chang, et al., Vascular anastomosis using controlled phase transitions in poloxamer gels, *Nat. Med.* 17 (2011) 1147–1152.
- [89] S. Nam, D. Mooney, Polymeric tissue adhesives, *Chem. Rev.* 121 (2021) 11336–11384.
- [90] H. Yuk, et al., Dry double-sided tape for adhesion of wet tissues and devices, *Nature* 575 (2019) 169–174.
- [91] G.-Y. Han, S.-K. Hwang, K.-H. Cho, H.-J. Kim, C.-S. Cho, Progress of tissue adhesives based on proteins and synthetic polymers, *Biomater. Res.* 27 (2023) 57.
- [92] Z. Bao, M. Gao, Y. Sun, R. Nian, M. Xian, The recent progress of tissue adhesives in design strategies, adhesive mechanism and applications, *Mater. Sci. Eng., C* 111 (2020) 110796.
- [93] A. Bal-Ozturk, et al., Tissue adhesives: from research to clinical translation, *Nano Today* 36 (2021).
- [94] E.I. Chang, et al., Vascular anastomosis using controlled phase transitions in poloxamer gels, *Nat. Med.* 17 (2011) 1147–1152.
- [95] X. Liang, S. Liu, Z. Fang, G. Sun, Z. Guo, Prevention of vascular anastomotic stenosis with 2-octylcyanoacrylate, *J. Craniofac. Surg.* 30 (2019) 74–80.
- [96] A.V. Orădan, et al., Reduction of anastomotic time through the use of cyanoacrylate in microvascular procedures, *Plastic Surg.* 30 (2021) 335–342.
- [97] T. Aizawa, et al., Sutureless microvascular anastomosis using intravascular stenting and cyanoacrylate adhesive, *J. Reconstr. Microsurg.* 34 (2018) 8–12.
- [98] A.B. Cho, et al., Fibrin glue application in microvascular anastomosis: comparative study of two free flaps series, *Microsurgery* 29 (2009) 24–28.
- [99] G.M. Dowbak, R.J. Rohrich, J.B. Robinson Jr., E. Peden, Effectiveness of a new non-thrombogenic bio-adhesive in microvascular anastomoses, *J. Reconstr. Microsurg.* 10 (1994) 383–386.
- [100] M. Le Hanneur, et al., Conventional versus fibrin-glue-augmented arterial microanastomosis: an experimental study, *Hand Surg. Rehab.* 41 (2022) 569–575.
- [101] D. Pacini, et al., BioGlue® is not associated with polypropylene suture breakage after aortic surgery, *Front. Surg.* 9 (2022).
- [102] A. Singh, L. Wales, Late sterile cyst formation following use of biogluce in carotid endarterectomy, *Eur. J. Vasc. Endovasc. Surg.* 58 (2019) e128.
- [103] S. Zaki, A. Khalaf, BioGlue: a nidus for late neck abscess after carotid endarterectomy, *Eur. J. Vasc. Endovasc. Surg.* 60 (2020) 450.
- [104] P. Slezak, et al., Tissue reactions to polyethylene glycol and glutaraldehyde-based surgical sealants in a rabbit aorta model, *J. Biomater. Appl.* 34 (2020) 1330–1340.
- [105] V. Dhandapani, V. Ringuette, M. Desrochers, M. Sirois, P. Vermette, Composition, host responses and clinical applications of bioadhesives, *J. Biomed. Mater. Res. B Appl. Biomater.* 110 (2022) 2779–2797.
- [106] M. Heitzer, et al., Evaluation of the long-term results of vascular anastomosis using polyurethane adhesive and shape-memory stent in the rat carotid artery model, *Microsurgery* 42 (2022) 480–489.
- [107] L. Schulten, et al., A polyurethane-based surgical adhesive for sealing blood vessel anastomoses-A feasibility study in pigs, *J. Biomed. Mater. Res. B Appl. Biomater.* 110 (2022) 1922–1931.
- [108] A. Modabber, et al., Biodegradation and immunological parameters of polyurethane-based tissue adhesive in arterial microvascular anastomoses-A long-term in vivo study, *Macromol. Biosci.* 22 (2022) e2100451.
- [109] D. Li, et al., Recent advances on synthetic and polysaccharide adhesives for biological hemostatic applications, *Front. Bioeng. Biotechnol.* 8 (2020) 926.
- [110] S. Luo, et al., Rapid suture-free repair of arterial bleeding: a novel approach with ultra-thin bioadhesive hydrogel membrane, *Chem. Eng. J.* 472 (2023) 144865.
- [111] K. Liu, et al., Adhesive anastomosis for organ transplantation, *Bioact. Mater.* 13 (2022) 260–268.
- [112] G.M. Taboada, et al., Overcoming the translational barriers of tissue adhesives, *Nat. Rev. Mater.* 5 (2020) 310–329.
- [113] A.V. Orădan, et al., Reduction of anastomotic time through the use of cyanoacrylate in microvascular procedures, *Plast Surg (Oakv)* 30 (2022) 335–342.
- [114] M. Brennan, Fibrin glue, *Blood Rev.* 5 (1991) 240–244.
- [115] H. Matras, The use of fibrin sealant in oral and maxillofacial surgery, *J. Oral Maxillofac. Surg.* 40 (1982) 617–622.
- [116] R.M. Pearl, K.O. Wustrack, C. Harbury, E. Rubenstein, E.N. Kaplan, Microvascular anastomosis using a blood product sealant-adhesive, *Surg. Gynecol. Obstet.* 144 (1977) 227–231.
- [117] H. Fonouni, et al., Analysis of the hemostatic potential of modern topical sealants on arterial and venous anastomoses: an experimental porcine study, *J. Mater. Sci. Mater. Med.* 28 (2017) 134.
- [118] M. Heitzer, et al., Evaluation of fibrin, cyanoacrylate, and polyurethane-based tissue adhesives in sutureless vascular anastomosis: a comparative mechanical ex vivo study, *Int. J. Oral Maxillofac. Surg.* 52 (2023) 1137–1144.
- [119] M. Heitzer, et al., Evaluation of the hemostatic effect of an innovative tissue adhesive during extraction therapy under rivaroxaban in a rodent model, *J. Funct. Biomater.* 14 (2023).
- [120] J. Liu, et al., Triggerable tough hydrogels for gastric resident dosage forms, *Nat. Commun.* 8 (2017) 124.
- [121] H. Yang, C. Li, J. Tang, Z. Suo, Strong and degradable adhesion of hydrogels, *ACS Appl. Bio Mater.* 2 (2019) 1781–1786.
- [122] M.C. Darnell, et al., Performance and biocompatibility of extremely tough alginate/polyacrylamide hydrogels, *Biomaterials* 34 (2013) 8042–8048.
- [123] N. Oliva, et al., Regulation of dendrimer/dextran material performance by altered tissue microenvironment in inflammation and neoplasia, *Sci. Transl. Med.* 7 (2015) 272ra211.
- [124] G. Muñoz Taboada, P. Dosta, E.R. Edelman, N. Artzi, Sprayable hydrogel for instant sealing of vascular anastomosis, *Adv. Mater.* 34 (2022) 2203087.
- [125] J. Wu, et al., Less-suture vascular anastomosis: development of alternative protocols with multifunctional self-wrapping, transparent, adhesive, and elastic biomaterials, *Adv. Mater.* 35 (2023) 2301098.
- [126] J. Ju, et al., Addressing the shortcomings of polyphenol-derived adhesives: achievement of long shelf life for effective hemostasis, *ACS Appl. Mater. Interfaces* 14 (2022) 25115–25125.
- [127] H.H. Shin, J.H. Ryu, Bio-inspired self-healing, shear-thinning, and adhesive gallic acid-conjugated chitosan/carbon black composite hydrogels as suture support materials, *Biomimetics* (2023), <https://doi.org/10.3390/biomimetics8070542>.
- [128] Y. Hong, et al., A strongly adhesive hemostatic hydrogel for the repair of arterial and heart bleeds, *Nat. Commun.* 10 (2019) 2060.
- [129] H. Ren, et al., Injectable, self-healing hydrogel adhesives with firm tissue adhesion and on-demand biodegradation for sutureless wound closure, *Sci. Adv.* 9 (2023) eadh4327.
- [130] Z. Zhang, et al., A fast and versatile cross-linking strategy via o-phthalaldehyde condensation for mechanically strengthened and functional hydrogels, *Nat. Sci. Rev.* 8 (2021) nwa128.
- [131] M. Gerressen, et al., Microsurgical free flap reconstructions of head and neck region in 406 cases: a 13-year experience, *J. Oral Maxillofac. Surg.* 71 (2013) 628–635.
- [132] K.T. Lee, J.E. Lee, S.J. Nam, G.H. Mun, Ischaemic time and fat necrosis in breast reconstruction with a free deep inferior epigastric perforator flap, *J. Plast. Reconstr. Aesthetic Surg.* 66 (2013) 174–181.
- [133] N.S. Hillberg, J. Beugels, S.M.J. van Kuijk, R.R.J.W. van der Hulst, S.M. H. Tuinder, Increase of major complications with a longer ischemia time in breast reconstruction with a free deep inferior epigastric perforator (DIEP) flap, *Eur. J. Plast. Surg.* 43 (2020) 133–138.
- [134] S. Ma, S. Duan, Y. Liu, H. Wang, Intimal hyperplasia of arteriovenous fistula, *Ann. Vasc. Surg.* 85 (2022) 444–453.
- [135] S. Déglise, C. Bechelli, F. Allagnat, Vascular smooth muscle cells in intimal hyperplasia, an update, *Front. Physiol.* 13 (2022) 1081881.
- [136] F.W. Bär, F.H. van der Veen, A. Benzina, J. Habets, L.H. Koole, New biocompatible polymer surface coating for stents results in a low neointimal response, *J. Biomed. Mater. Res.* 52 (2000) 193–198.
- [137] P. Tozzi, Sutureless anastomoses, Secrets for success. Sutureless Anastomoses: Secrets for Success, 2007, pp. 1–140.
- [138] K.K. Wu, P. Thiagarajan, Role of endothelium in thrombosis and hemostasis, *Annu. Rev. Med.* 47 (1996) 315–331.
- [139] P. Libby, D.I. Simon, Inflammation and thrombosis: the clot thickens, *Circulation* 103 (2001) 1718–1720.

- [140] J. Cermak, et al., C-reactive protein induces human peripheral blood monocytes to synthesize tissue factor, *Blood* 82 (1993) 513–520.
- [141] R.J. Bisioendial, et al., Activation of inflammation and coagulation after infusion of C-reactive protein in humans, *Circ. Res.* 96 (2005) 714–716.
- [142] S. Mok, et al., Optimizing venous anastomosis angle for arteriovenous graft with intimal hyperplasia using computational fluid dynamics, *J. Mech. Sci. Technol.* 37 (2023) 5231–5238.
- [143] D. Williams, E.C. Leuthardt, G.M. Genin, M. Zayed, Tailoring of arteriovenous graft-to-vein anastomosis angle to attenuate pathological flow fields, *Sci. Rep.* 11 (2021) 12153.
- [144] J.J. Paszkowiak, A. Dardik, Arterial wall shear stress: observations from the bench to the bedside, *Vasc. Endovasc. Surg.* 37 (2003) 47–57.
- [145] J.J. Hathcock, Flow effects on coagulation and thrombosis, *Arterioscler. Thromb. Vasc. Biol.* 26 (2006) 1729–1737.
- [146] J.J. Chiu, S. Chien, Effects of disturbed flow on vascular endothelium: pathophysiological basis and clinical perspectives, *Physiol. Rev.* 91 (2011) 327–387.
- [147] A. Saito, et al., The relationship between coronary stent strut thickness and the incidences of clinical outcomes after drug-eluting stent implantation: a systematic review and meta-regression analysis, *Cathet. Cardiovasc. Interv.* 99 (2022) 575–582.
- [148] J. Ng, et al., Local hemodynamic forces after stenting: implications on restenosis and thrombosis, *Arterioscler. Thromb. Vasc. Biol.* 37 (2017) 2231–2242.
- [149] H. Wang, et al., Three-dimensional virtual surgery models for percutaneous coronary intervention (PCI) optimization strategies, *Sci. Rep.* 5 (2015) 10945.
- [150] J. Mejia, B. Ruzzeh, R. Mongrain, R. Leask, O.F. Bertrand, Evaluation of the effect of stent strut profile on shear stress distribution using statistical moments, *Biomed. Eng. Online* 8 (2009) 8.
- [151] J.M. Jiménez, P.F. Davies, Hemodynamically driven stent strut design, *Ann. Biomed. Eng.* 37 (2009) 1483–1494.
- [152] K. Kollandaivelu, et al., Stent thrombogenicity early in high-risk interventional settings is driven by stent design and deployment and protected by polymer-drug coatings, *Circulation* 123 (2011) 1400–1409.
- [153] Q. Han, S.M. Shea, T. Arleo, J.Y. Qian, D.N. Ku, Thrombogenicity of biomaterials depends on hemodynamic shear rate, *Artif. Organs* 46 (2022) 606–617.
- [154] FDA, The device development process. <https://www.fda.gov/medical-devices/device-advice-comprehensive-regulatory-assistance/overview-device-regulation>, 2023.
- [155] FDA, Premarket Approval (PMA). <https://www.fda.gov/medical-devices/premarket-submissions-selecting-and-preparing-correct-submission/premarket-approval-pma>.
- [156] E. Pace, B. Mast, J.M. Pierson, A. Leavitt, C. Reintgen, Evolving perceptions of the plastic surgery integrated residency training program, *J. Surg. Educ.* 73 (2016) 799–806.
- [157] Y.-J. Wang, X.-L. Wang, S. Jin, R. Zhang, Y.-Q. Gao, Meta-analysis of arterial anastomosis techniques in head and neck free tissue transfer, *PLoS One* 16 (2021) e0249418.
- [158] K. Kania, et al., Microsurgery training in plastic surgery, *Plast. Reconstr. Surg. Glob. Open* 8 (2020) e2898.
- [159] J.A. Henry, O. Windapo, A.L. Kushner, R.S. Groen, B.C. Nwomeh, A survey of surgical capacity in rural southern Nigeria: opportunities for change, *World J. Surg.* 36 (2012) 2811–2818.
- [160] S. Yiltok, Plastic surgery in Nigeria: our yesterday, today and tomorrow, *Nigerian J. Plastic Surg.* 16 (2020) 1–8.
- [161] D.S. Corlew, Perspectives on plastic surgery and global health, *Ann. Plast. Surg.* 62 (2009).
- [162] J. Chen, et al., Predictors and consequences of intraoperative anastomotic failure in DIEP flaps, *J. Reconstr. Microsurg.* (2022).
- [163] R.B. Iamaguchi, et al., Microsurgical reconstruction in an orthopedic hospital: indications and outcomes in adults, *Rev. Bras Ortop. (Sao Paulo)* 57 (2022) 772–780.
- [164] F. Kabirian, et al., Controlled NO-release from 3D-printed small-diameter vascular grafts prevents platelet activation and bacterial infectivity, *ACS Biomater. Sci. Eng.* 5 (2019) 2284–2296.
- [165] R. Khalaj, A.G. Tabriz, M.I. Okereke, D. Douroumis, 3D printing advances in the development of stents, *Int. J. Pharm.* 609 (2021) 121153.
- [166] J.E. Hull, B.V. Balakin, B.M. Kellerman, D.K. Wrolstad, Computational fluid dynamic evaluation of the side-to-side anastomosis for arteriovenous fistula, *J. Vasc. Surg.* 58 (2013) 187–193, e181.
- [167] R.A.J. Wain, N.J. Gaskell, A.M. Fsadni, J. Francis, J.P.M. Whitty, Finite element predictions of sutured and coupled microarterial anastomoses, *Adv. Biomed. Eng.* 8 (2019) 63–77.
- [168] S. Yagi, et al., Hemodynamic analysis of a microanastomosis using computational fluid dynamics, *Yonago Acta Med.* 63 (2020) 308–312.